Convergence analysis of a BDF finite element method for the resistive magnetohydrodynamic equations

Lina Ma*, Cheng Wang†, Zeyu Xia‡

August 30, 2023

Abstract

In this paper we propose and analyze a numerical scheme coupling a second-order backward differential formulation (BDF) and the finite element method (FEM) to solve the incompressible resistive magnetohydrodynamic (MHD) equations. In the discrete scheme, the pressure variable in the fluid field equation is computed through a Poisson equation, and a linear and decoupled method is adopted to separate both the magnetic and the fluid field functions from the original system. As a result, the original system is divided into several sub-systems for which the numerical solutions can be obtained efficiently. We prove the unique solvability, the unconditional energy stability, and particularly optimal error estimates for the proposed scheme. Numerical results are presented to validate the theory of the scheme.

Keywords: Resistive MHD equations, finite element methods, BDF decoupled scheme, unconditional energy stability, optimal error estimates.
MSC: 65M60, 65M12

1 Introduction

The MHD system describes the interaction between the conductive fluids and the electromagnetic fields [16]. It has been widely applied to the industry production, such as liquid-metal processing, and its numerical solutions are of great significance in science and engineering [45]. This model is governed by the Navier–Stokes equations and the Maxwell equations through the Ohm's law and the Lorentz force. Physically, in order to consider the further effect of magnetic fields, one can introduce a fourth-order curl operator on the magnetic fields into the standard incompressible MHD equations, arriving at the following so-called incompressible resistive MHD system [65]

$$\partial_t \boldsymbol{H} - \nabla \times (\boldsymbol{u} \times \boldsymbol{H}) + \frac{\eta}{\mu_0} \nabla \times (\nabla \times \boldsymbol{H}) + \frac{\eta_2}{\mu_0} \nabla \times (\nabla \times (\nabla \times (\nabla \times \boldsymbol{H}))) = \boldsymbol{0}, \tag{1.1}$$

$$\partial_t \boldsymbol{u} + \boldsymbol{u} \cdot \nabla \boldsymbol{u} - \mu \Delta \boldsymbol{u} + \nabla p + \frac{1}{\mu_0} \boldsymbol{H} \times (\nabla \times \boldsymbol{H}) = \boldsymbol{0}, \tag{1.2}$$

$$\nabla \cdot \boldsymbol{u} = 0, \tag{1.3}$$

over $\Omega \times (0, T]$, where Ω is a bounded and convex polygonal domain in $\mathbb{R}^2$ (polyhedral domain in $\mathbb{R}^3$), and T is a constant representing the final time. Here, the unknowns $\boldsymbol{u}$, $\boldsymbol{H}$ and p denote the velocity field, the magnetic filed, and the pressure variable, respectively. The constant η represents the resistivity, η_2 is the

*Department of Mathematics, Trinity College, Hartford, CT 06106, USA. Email: lina.ma@trincoll.edu
†Mathematics Department, University of Massachusetts, North Dartmouth, MA 02747, USA. Email: cwang1@umassd.edu
‡School of Science, Harbin Institute of Technology, Shenzhen 518055, China. Email: xiazeyu@hit.edu.cn

hyper-resistivity, μ is the viscosity of the fluid and μ_0 stands for the magnetic permeability of free space. The initial and boundary conditions are given by

$$\boldsymbol{H}|_{t=0} = \boldsymbol{H}_0, \quad \boldsymbol{u}|_{t=0} = \boldsymbol{u}_0, \qquad \text{in } \Omega, \tag{1.4}$$
$$\boldsymbol{H} \times \boldsymbol{n} = \boldsymbol{0}, \quad (\nabla \times (\nabla \times \boldsymbol{H})) \times \boldsymbol{n} = \boldsymbol{0}, \quad \boldsymbol{u} = \boldsymbol{0}, \qquad \text{on } \partial\Omega \times (0, T]. \tag{1.5}$$

It is assumed that the initial data satisfies

$$\nabla \cdot \boldsymbol{H}_0 = \nabla \cdot \boldsymbol{u}_0 = 0. \tag{1.6}$$

By taking the divergence of (1.1), we have $\partial_t \nabla \cdot \boldsymbol{H} = 0$, which together with the above divergence-free initial condition indicates that $\nabla \cdot \boldsymbol{H} = 0$ for any $t > 0$.

Apparently, taking hyper-resistivity coefficient $\eta_2 = 0$ would reduce the original system (1.1)-(1.3) into the standard incompressible MHD system. There have been already many works dedicated to regularity analysis of the incompressible MHD system [23,36,37,48]. Concerning finite element methods for the MHD system, many research efforts have been devoted to the use of the $H^1(\Omega)$ conforming elements, since the weak solutions of the system are located in $H^1(\Omega)$. In [22], Gunzburger et al. proposed a numerical scheme and analyzed optimal error estimates for the stationary MHD system by $H^1(\Omega)$ conforming elements. The similar results were obtained for the time-dependent MHD model in [24]. Li et al. developed a strongly convergent finite element scheme based on the $H^1(\Omega)$ conforming elements in general domains, which may be nonconvex, nonsmooth and multi-connected, without any mesh restriction [30]. Wang et al. designed a second-order temporally accurate finite element scheme with the $H^1(\Omega)$ conforming elements, and provided a rigorous proof on optimal error estimates [47]. More works about $H^1(\Omega)$ conforming elements are referred to [25, 47, 52, 58, 60] and references therein. An apparent difference between the standard MHD system and the resistive MHD system is the appearance of the fourth-order curl operator, for which many numerical schemes have been proposed and analyzed. Zheng et al. utilized a non-conforming finite element involving a small number of degrees of freedom for its solution [65]. Sun proposed a mixed finite element method by introducing an intermediate variable $\boldsymbol{\phi} = \nabla \times (\nabla \times \boldsymbol{H})$, and proved the unique solvability and the convergence for the proposed scheme [43]. Discontinuous Galerkin (DG) methods with $H(\text{curl})$-conforming elements were adopted to solve the fourth-order curl operator problem in [26]. Both an interior penalty DG method and a hybridizable discontinuous Galerkin (HDG) method were employed to discretize this operator in [7] and [5,6], respectively. Most recently, Zhang et al. developed the two-dimensional $H(\text{curl}^2)$-conforming finite elements on both rectangles and triangles, and applied them to solve this operator, with the convergence rates being proved [63]. In [27], three families of finite elements, among which the simplest triangular or rectangular finite elements have only six or eight degrees of freedom, respectively, have been constructed in two dimensions to solve this fourth-order curl operator problem.

On the design of fully discrete schemes for the time-dependent incompressible MHD system, there exist issues on treating both the divergence-free condition on the magnetic fields and the incompressibility constraint. There are many works devoted to the construction of divergence-free schemes for the MHD equations, and interested readers are referred to such as [31–33]. Dealing with the incompressibility constraint, a type of numerical schemes is based on the Stokes solver, which leads to a coupling of the pressure gradient and the incompressibility constraint at each time step, for example in [20, 24]. As a result, this method will generate a non-symmetric system. Another type of approaches is to making use of the "decoupled" technique. An advantage of this method, being friendly to the improvement on computational efficiency, can be attained due to the fact that the resulting discrete system is symmetric. In [42], Pyo and Shen have proposed a second-order decoupled BDF scheme for the incompressible Navier–Stokes equations, and also see [46] for the decoupled fluid solver using the Gauge formulation. In [38], Liu et al. designed a decoupled scheme with the first-order temporally accuracy and unconditional energy stability for a phase-field model of two-phase incompressible flows with variable density based on the "pressure-stabilized" formulation, in which they treated the pressure term in the velocity equation explicitly and then computed the pressure by solving a Poisson equation. Zhao et al. proposed a decoupled, linear and first-order temporally accurate scheme with the unconditional stability analysis for the phase field model of mixtures of nematic liquid crystals and viscous fluids [64]. The emphasis of these works related to the "decoupled" technique was concentrated on the energy-preserving property but not on the convergence analysis. Meanwhile, there have been some works devoted to the improvement on the computational efficiency through particularly dealing with the nonlinear and coupled terms in the complex system. In addition to the general im-explicit technique, a novel approach being called the "zero-energy-contribution" property has been developed recently. In [62], Zhang et. al. designed a fully decoupled scheme for the incompressible MHD with second-order temporal accuracy and unconditional energy stability. More works applying the "zero-energy-contribution" property could be found in [53–57, 61] and the references therein. However, the existing fully decoupled schemes using the "zero-energy-contribution" property have only addressed the stability analysis, without accuracy analysis being presented. Moreover, for the time-dependent problem, to improve the computational efficiency the various time step method, e.g. [9] and the SAV method e.g., [35] are also feasible. In particular, the "zero-energy-contribution" method shares a little similar ideas of the SAV method, where the primary difference is the definition of the nonlocal artificial variable.

In this work, we design a numerical scheme of the FEM approximation in spatial domain and a second-order BDF discretization in time domain to solve the resistive MHD system. The scheme has a feature of fully decoupling making use of both the "pressure-stabilized" formulation and the "zero-energy-contribution" property. By defining an intermediate variable $\boldsymbol{\phi} = \nabla \times (\nabla \times \boldsymbol{H})$, the original resistive MHD system (1.1)-(1.3) can be reformulated, and the equivalence holds since we consider the problem only in convex domains. In the discrete scheme, we employ the $H^1(\Omega)$-conforming elements, the "decoupled" method combined with the second-order BDF scheme, and the "zero-energy-contribution" property dealing with the nonlinear terms. This approach ensures the linear nature of the fully discrete system, and then the unique solvability follows immediately from the fact that the corresponding homogeneous equation only admits a trivial solution. We point out that the second order accurate temporal discretization has been applied to various gradient flow models [10–12, 17, 19, 34, 39, 51, 59], with the energy stability and the convergence estimate being theoretically proved. During the numerical implementation, we carry out the implementation step by step, instead of solving the full system together, and consequently, the conjugate gradient method could be applied to compute the velocity field, and the pressure is obtained by solving a Poisson-type equation. In order to validate the analysis on the artificial velocity field, we introduce the corresponding artificial projection operators and assume that the pressure field satisfies $\nabla p = 0$ on the boundary [47]. We carry out a rigorous analysis on the unconditional energy stability, the unique solvability, and particularly the optimal error estimate for the scheme. The numerical scheme has the feature of the optimal convergence rate $O(h^{r+1} + \tau^2)$, in the $\ell^\infty([0,T], L^2)$-norm, where r is the degree of the polynomial functions, and h and τ are the spatial and temporal sizes, respectively.

This paper is organized as follows. In Section 2 we present the variational formulation of the resistive MHD system, and then discuss the numerical scheme and its the theoretical results, including the energy stability and the unique solvability in Section 3. In Section 4, the convergence analysis and the optimal error estimates for the scheme are established, and finally some numerical results are presented in Section 5 to verify the theoretic results.

2 Variational formulation

We adopt the standard Sobolev space $W^{k,p}(\Omega)$ of functions defined on Ω for $k \geqslant 0$ and $1 \leqslant p \leqslant \infty$, and denote $L^p(\Omega) = W^{0,p}(\Omega)$ and $H^k(\Omega) = W^{k,2}(\Omega)$. Then we take the notation $W_0^{1,p}(\Omega)$ as the space of functions in $W^{1,p}(\Omega)$ with zero traces on the boundary $\partial\Omega$, and naturally $H_0^1(\Omega) := W_0^{1,2}(\Omega)$. The corresponding vector spaces are given by

$$
\begin{aligned}
&\mathbf{L}^p(\Omega) = [L^p(\Omega)]^d, && \mathbf{W}^{k,p}(\Omega) = [W^{k,p}(\Omega)]^d,\\
&\mathbf{W}_0^{1,p}(\Omega) = [W_0^{1,p}(\Omega)]^d, && \mathbf{H}_0^1(\Omega) = \mathbf{W}_0^{1,2}(\Omega),\\
&\mathring{\mathbf{H}}^k(\Omega) = \{\boldsymbol{v} \in \mathbf{H}^k(\Omega) : \boldsymbol{v} \times \boldsymbol{n} = 0\},
\end{aligned}
$$

where d denotes the dimension of space. As usual, $(\cdot,\cdot)$ denotes the inner product in $L^2(\Omega)$.

We introduce an intermediate variable $\boldsymbol{\phi} = \nabla \times (\nabla \times \boldsymbol{H})$ [43] in (1.1) to reformulate the original system (1.1)-(1.3), and additionally define another artificial nonlocal variable M_e [62] satisfying the following initial value problem

$$
\frac{dM_e}{dt} = -(\boldsymbol{u} \times \boldsymbol{H}, \nabla \times \boldsymbol{H}) + \mu_0 b(\boldsymbol{u},\boldsymbol{u},\boldsymbol{u}) + (\boldsymbol{H} \times (\nabla \times \boldsymbol{H}), \boldsymbol{u}), \quad M_e(0) = 1. \tag{2.1}
$$

Here, we define a trilinear operator $b(\cdot,\cdot,\cdot)$ as follows

$$
\begin{aligned}
b(\boldsymbol{u},\boldsymbol{v},\boldsymbol{w}) :&= (\boldsymbol{u}\cdot\nabla\boldsymbol{v},\boldsymbol{w}) + \frac{1}{2}((\nabla\cdot\boldsymbol{u})\boldsymbol{v},\boldsymbol{w})\\
&= \frac{1}{2}\big[(\boldsymbol{u}\cdot\nabla\boldsymbol{v},\boldsymbol{w}) - (\boldsymbol{u}\cdot\nabla\boldsymbol{w},\boldsymbol{v})\big], \quad \forall \boldsymbol{u},\boldsymbol{v},\boldsymbol{w} \in \mathbf{H}_0^1(\Omega),
\end{aligned} \tag{2.2}
$$

and obviously we have

$$
b(\boldsymbol{u},\boldsymbol{v},\boldsymbol{v}) = 0, \quad \forall \boldsymbol{u},\boldsymbol{v} \in \mathbf{H}_0^1(\Omega). \tag{2.3}
$$

It can be easily seen that $M_e \equiv 1$ for any $t > 0$ by integration by parts with boundary conditions (1.5).

Turning to these new variables, we can reformulate the original system (1.1)-(1.3) into

$$
\begin{aligned}
&\partial_t \boldsymbol{H} - M_e \nabla \times (\boldsymbol{u} \times \boldsymbol{H}) + \frac{\eta}{\mu_0}\nabla \times (\nabla \times \boldsymbol{H}) + \frac{\eta_2}{\mu_0}\nabla \times (\nabla \times \boldsymbol{\phi}) = \mathbf{0},\\
&\nabla \times (\nabla \times \boldsymbol{H}) = \boldsymbol{\phi},\\
&\partial_t \boldsymbol{u} + M_e \boldsymbol{u}\cdot\nabla\boldsymbol{u} - \mu\Delta\boldsymbol{u} + \nabla p + \frac{M_e}{\mu_0}\boldsymbol{H} \times (\nabla \times \boldsymbol{H}) = \mathbf{0},\\
&\nabla\cdot\boldsymbol{u} = 0,
\end{aligned}
$$

which leads to the following variational formulation: find $(\boldsymbol{H},\boldsymbol{\phi},\boldsymbol{u},p) \in (\mathring{\mathbf{H}}^1(\Omega), \mathring{\mathbf{H}}^1(\Omega), \mathbf{H}_0^1(\Omega), L^2(\Omega))$ such that it holds

$$
(\partial_t \boldsymbol{H}, \boldsymbol{w}) - M_e(\boldsymbol{u} \times \boldsymbol{H}, \nabla \times \boldsymbol{w}) + \frac{\eta}{\mu_0}(\nabla \times \boldsymbol{H}, \nabla \times \boldsymbol{w}) + \frac{\eta_2}{\mu_0}(\nabla \times \boldsymbol{\phi}, \nabla \times \boldsymbol{w}) = 0, \tag{2.4}
$$

$$
(\nabla \times \boldsymbol{H}, \nabla \times \boldsymbol{v}) - (\boldsymbol{\phi}, \boldsymbol{v}) = 0, \tag{2.5}
$$

$$
(\partial_t \boldsymbol{u}, \boldsymbol{l}) + M_e b(\boldsymbol{u},\boldsymbol{u},\boldsymbol{l}) + \mu(\nabla\boldsymbol{u}, \nabla\boldsymbol{l}) - (p, \nabla\cdot\boldsymbol{l}) + \frac{M_e}{\mu_0}(\boldsymbol{H} \times (\nabla \times \boldsymbol{H}), \boldsymbol{l}) = 0, \tag{2.6}
$$

$$
(\nabla\cdot\boldsymbol{u}, q) = 0, \tag{2.7}
$$

for any test functions $(\boldsymbol{w},\boldsymbol{v},\boldsymbol{l},q) \in (\mathring{\mathbf{H}}^1(\Omega), \mathring{\mathbf{H}}^1(\Omega), \mathbf{H}_0^1(\Omega), L^2(\Omega))$.

Remark 2.1. *The intermediate variable $\boldsymbol{\phi} = \nabla \times (\nabla \times \boldsymbol{H})$ is an auxiliary function served for computation and analysis, and it is assumed that it also satisfies the boundary condition $\boldsymbol{\phi} \times \boldsymbol{n} = 0$. This assumption for now does not contain the physical meaning, and we mainly focus on the theoretical analysis in this work, so that the simple boundary conditions are discussed.*

It is a well-known technique through introducing an artificial variable to reduce the order of the original system in the process of designing numerical schemes, such as mixed finite element methods [1–3, 8, 13, 40] and local discontinuous Galerkin methods [15, 29, 49, 50]. In this work we mainly focus on the theoretical analysis, so that the simple boundary conditions are discussed.

3 Numerical methods and stability analysis

3.1 Discrete scheme

We divide the domain Ω into triangles K_j (tetrahedrons K_j in $\mathbb{R}^3$), $j = 1, 2, \ldots, N_x$, denoted by $\Im_h$, and the mesh size is defined as $h = \max_{1\leqslant j\leqslant N_x}\{\mathrm{diam}K_j\}$. We utilize the Taylor-Hood finite element, given by

$$\mathbf{X}_h = \{\boldsymbol{l}_h \in \mathbf{H}_0^1(\Omega) : \boldsymbol{l}_h|_{K_j} \in \mathbf{P}_r(K_j)\},$$
$$Q_h = \{q_h \in L^2(\Omega) : q_h|_{K_j} \in P_{r-1}(K_j),\ \textstyle\int_\Omega q_h \boldsymbol{dx} = 0\},$$

for any integer $r \geqslant 2$, where $P_r(K_j)$ is the polynomial space with the degree being r on K_j for all $K_j \in \Im_h$ and $\mathbf{P}_r(K_j) := [P_r(K_j)]^d$. Additionally, we introduce the finite element space $\mathbf{S}_h$:

$$\mathbf{S}_h = \{\boldsymbol{w}_h \in \mathring{\mathbf{H}}^1(\Omega) : \boldsymbol{w}_h|_{K_j} \in \mathbf{P}_r(K_j)\}.$$

Let $\{t_n = n\tau\}_{n=0}^N$ be a uniform partition of the time interval $[0, T]$, and $\tau = T/N$ denotes the temporal step size. Furthermore, v^n represents the value of $v(x, t_n)$, and for any sequences $\{v^n\}_{n=1}^N$ we define

$$\widetilde{v}^{n+1} := 2v^n - v^{n-1}.$$

Subsequently, based on (2.1) and (2.4)-(2.7), we propose a fully discrete scheme for the incompressible resistive MHD equations (1.1)-(1.3): find $(\boldsymbol{H}_h^{n+1}, \boldsymbol{\phi}_h^{n+1}, \boldsymbol{u}_h^{n+1}, \hat{\boldsymbol{u}}_h^{n+1}, p_h^{n+1}) \in (\mathbf{S}_h, \mathbf{S}_h, \mathbf{X}_h, \mathbf{X}_h, Q_h)$ together with M^{n+1} such that

$$\begin{aligned}
&\Big(\frac{3\boldsymbol{H}_h^{n+1} - 4\boldsymbol{H}_h^n + \boldsymbol{H}_h^{n-1}}{2\tau}, \boldsymbol{w}_h\Big) + \frac{\eta}{\mu_0}\big(\nabla \times \boldsymbol{H}_h^{n+1}, \nabla \times \boldsymbol{w}_h\big) + \frac{\eta}{\mu_0}\big(\nabla \cdot \boldsymbol{H}_h^{n+1}, \nabla \cdot \boldsymbol{w}_h\big)\\
&\quad + \frac{\eta_2}{\mu_0}\big(\nabla \times \boldsymbol{\phi}_h^{n+1}, \nabla \times \boldsymbol{w}_h\big) + \frac{\eta_2}{\mu_0}\big(\nabla \cdot \boldsymbol{\phi}_h^{n+1}, \nabla \cdot \boldsymbol{w}_h\big) - M^{n+1}\big(\tilde{\boldsymbol{u}}_h^{n+1} \times \widetilde{\boldsymbol{H}}_h^{n+1}, \nabla \times \boldsymbol{w}_h\big) = 0, &(3.1)\\
&\big(\nabla \times \boldsymbol{H}_h^{n+1}, \nabla \times \boldsymbol{v}_h\big) + \big(\nabla \cdot \boldsymbol{H}_h^{n+1}, \nabla \cdot \boldsymbol{v}_h\big) - \big(\boldsymbol{\phi}_h^{n+1}, \boldsymbol{v}_h\big) = 0, &(3.2)\\
&\Big(\frac{3\hat{\boldsymbol{u}}_h^{n+1} - 4\boldsymbol{u}_h^n + \boldsymbol{u}_h^{n-1}}{2\tau}, \boldsymbol{l}_h\Big) + M^{n+1}b\big(\tilde{\boldsymbol{u}}_h^{n+1}, \tilde{\boldsymbol{u}}_h^{n+1}, \boldsymbol{l}_h\big) + \mu\big(\nabla\hat{\boldsymbol{u}}_h^{n+1}, \nabla \boldsymbol{l}_h\big) - \big(p_h^n, \nabla \cdot \boldsymbol{l}_h\big)\\
&\qquad + \frac{M^{n+1}}{\mu_0}\big(\widetilde{\boldsymbol{H}}_h^{n+1} \times (\nabla \times \widetilde{\boldsymbol{H}}_h^{n+1}), \boldsymbol{l}_h\big) = 0, &(3.3)\\
&\Big(\frac{\boldsymbol{u}_h^{n+1} - \hat{\boldsymbol{u}}_h^{n+1}}{\tau}, \boldsymbol{r}_h\Big) - \frac{2}{3}\big(p_h^{n+1} - p_h^n, \nabla \cdot \boldsymbol{r}_h\big) = 0, &(3.4)\\
&\big(\nabla \cdot \boldsymbol{u}_h^{n+1}, q_h\big) = 0, &(3.5)\\
&\frac{3M^{n+1} - 4M^n + M^{n-1}}{2\tau} = \big(\widetilde{\boldsymbol{H}}_h^{n+1} \times (\nabla \times \widetilde{\boldsymbol{H}}_h^{n+1}), \hat{\boldsymbol{u}}_h^{n+1}\big) + \mu_0 b\big(\tilde{\boldsymbol{u}}_h^{n+1}, \tilde{\boldsymbol{u}}_h^{n+1}, \hat{\boldsymbol{u}}_h^{n+1}\big)\\
&\qquad - \big(\tilde{\boldsymbol{u}}_h^{n+1} \times \widetilde{\boldsymbol{H}}_h^{n+1}, \nabla \times \boldsymbol{H}_h^{n+1}\big), &(3.6)
\end{aligned}$$

for any $(\boldsymbol{w}_h, \boldsymbol{v}_h, \boldsymbol{l}_h, \boldsymbol{r}_h, q_h) \in (\mathbf{S}_h, \mathbf{S}_h, \mathbf{X}_h, \mathbf{X}_h, Q_h)$ and $n = 1, 2, \ldots, N - 1$.

Remark 3.1. *We have added the stabilization terms, $\frac{\eta}{\mu_0}(\nabla \cdot \boldsymbol{H}_h^{n+1}, \nabla \cdot \boldsymbol{w}_h)$ and $\frac{\eta_2}{\mu_0}(\nabla \cdot \boldsymbol{\phi}_h^{n+1}, \nabla \cdot \boldsymbol{w}_h)$, to (3.1), and $\big(\nabla \cdot \boldsymbol{H}_h^{n+1}, \nabla \cdot \boldsymbol{v}_h\big)$ to (3.2), which are consistent with the conditions that $\nabla \cdot \boldsymbol{H} = 0$ and $\nabla \cdot \boldsymbol{\phi} = 0$. This manipulation, which has also been discussed in many literatures, e.g., [18, 28], allows us to utilize the H^1-conforming elements to validate the analysis on the optimal error estimate for the magnetic field in the convex domain. However, for the non-convex domains, one could use some advanced elements [41] to obtain the optimal rates, or other analysis techniques [30] to obtain the convergence results.*

Remark 3.2. *The pressure field appears explicitly in the velocity equation* (3.3)*, and it could be updated by solving the linear equation* (3.4)*. To this end, we also introduce an artificial variable* $\hat{\boldsymbol{u}}_h^{n+1}$ *instead of* $\boldsymbol{u}_h^{n+1}$ *in* (3.3)*, and then* $\boldsymbol{u}_h^{n+1}$ *will be obtained together with* p_h^{n+1} *in* (3.4)*. This is the so-called "pressure-stabilized" technique.*

Remark 3.3. *Note that the proposed scheme* (3.1)-(3.6) *is a multi-step method, and we simply assume that the initial values at* t^0 *and* t^1 *are given.*

3.2 Discrete energy stability

In this subsection, the discrete energy stability of the numerical scheme (3.1)-(3.6) will be proven. We define the discrete gradient operator $\nabla_h : Q_h \to \mathbf{X}_h$ as

$$(\boldsymbol{v}_h, \nabla_h q_h) = -(\nabla \cdot \boldsymbol{v}_h, q_h), \quad \forall \boldsymbol{v}_h \in \mathbf{X}_h, q_h \in Q_h. \tag{3.7}$$

The energy stability estimate is stated in the following theorem.

Theorem 3.4. *The numerical solution* $(\boldsymbol{H}_h^n, \boldsymbol{u}_h^n, p_h^n)$ *to the fully discrete scheme* (3.1)-(3.6) *is uniquely solvable and satisfies the following energy estimate*

$$\varepsilon_h^{n+1} \leqslant \varepsilon_h^n,$$

for $1 \leqslant n \leqslant N-1$*, where the discrete energy function* ε_h^n *is defined as*

$$\begin{aligned}\varepsilon_h^n =& \frac{1}{4}(\|\boldsymbol{H}_h^n\|_{L^2}^2 + \|2\boldsymbol{H}_h^n - \boldsymbol{H}_h^{n-1}\|_{L^2}^2 + \mu_0\|\boldsymbol{u}_h^n\|_{L^2}^2 + \mu_0\|2\boldsymbol{u}_h^n - \boldsymbol{u}_h^{n-1}\|_{L^2}^2 + (M^n)^2 \\ &+ (2M^n - M^{n-1})^2) + \frac{\mu_0\tau^2}{3}\|\nabla_h p_h^n\|_{L^2}^2.\end{aligned}$$

Proof. <u>*Step 1:*</u> Setting $\boldsymbol{w}_h = \boldsymbol{H}_h^{n+1}$ in (3.1) leads to

$$\begin{aligned}&\Big(\frac{3\boldsymbol{H}_h^{n+1} - 4\boldsymbol{H}_h^n + \boldsymbol{H}_h^{n-1}}{2\tau}, \boldsymbol{H}_h^{n+1}\Big) + \frac{\eta}{\mu_0}\|\nabla \times \boldsymbol{H}_h^{n+1}\|_{L^2}^2 + \frac{\eta}{\mu_0}\|\nabla \cdot \boldsymbol{H}_h^{n+1}\|_{L^2}^2 \\ &+ \frac{\eta_2}{\mu_0}(\nabla \times \boldsymbol{\phi}_h^{n+1}, \nabla \times \boldsymbol{H}_h^{n+1}) + \frac{\eta_2}{\mu_0}(\nabla \cdot \boldsymbol{\phi}_h^{n+1}, \nabla \cdot \boldsymbol{H}_h^{n+1}) - M^{n+1}\big(\tilde{\boldsymbol{u}}_h^{n+1} \times \widetilde{\boldsymbol{H}}_h^{n+1}, \nabla \times \boldsymbol{H}_h^{n+1}\big) = 0.\end{aligned}$$

Substituting $\boldsymbol{v}_h = \boldsymbol{\phi}_h^{n+1}$ into (3.2) gives

$$(\nabla \times \boldsymbol{\phi}_h^{n+1}, \nabla \times \boldsymbol{H}_h^{n+1}) + (\nabla \cdot \boldsymbol{\phi}_h^{n+1}, \nabla \cdot \boldsymbol{H}_h^{n+1}) = \|\boldsymbol{\phi}_h^{n+1}\|_{L^2}^2,$$

which together with the identity

$$(\frac{3}{2}a - 2b + \frac{1}{2}c)a = \frac{1}{4}[a^2 - b^2 + (2a-b)^2 - (2b-c)^2 + (a-2b+c)^2]$$

indicates that

$$\begin{aligned}&\frac{1}{4\tau}(\|\boldsymbol{H}_h^{n+1}\|_{L^2}^2 - \|\boldsymbol{H}_h^n\|_{L^2}^2 + \|2\boldsymbol{H}_h^{n+1} - \boldsymbol{H}_h^n\|_{L^2}^2 - \|2\boldsymbol{H}_h^n - \boldsymbol{H}_h^{n-1}\|_{L^2}^2) \\ &\qquad - M^{n+1}\big(\tilde{\boldsymbol{u}}_h^{n+1} \times \widetilde{\boldsymbol{H}}_h^{n+1}, \nabla \times \boldsymbol{H}_h^{n+1}\big) \leqslant 0.\end{aligned} \tag{3.8}$$

<u>*Step 2:*</u> Similarly, taking $\boldsymbol{l}_h = \hat{\boldsymbol{u}}_h^{n+1}$ in (3.3) yields

$$\begin{aligned}&\frac{1}{4\tau}(\|\hat{\boldsymbol{u}}_h^{n+1}\|_{L^2}^2 - \|\boldsymbol{u}_h^n\|_{L^2}^2 + \|2\hat{\boldsymbol{u}}_h^{n+1} - \boldsymbol{u}_h^n\|_{L^2}^2 - \|2\boldsymbol{u}_h^n - \boldsymbol{u}_h^{n-1}\|_{L^2}^2) - \big(p_h^n, \nabla \cdot \hat{\boldsymbol{u}}_h^{n+1}\big) \\ &+ M^{n+1} b\big(\tilde{\boldsymbol{u}}_h^{n+1}, \tilde{\boldsymbol{u}}_h^{n+1}, \hat{\boldsymbol{u}}_h^{n+1}\big) + \frac{M^{n+1}}{\mu_0}\big(\widetilde{\boldsymbol{H}}_h^{n+1} \times (\nabla \times \widetilde{\boldsymbol{H}}_h^{n+1}), \hat{\boldsymbol{u}}_h^{n+1}\big) \leqslant 0,\end{aligned} \tag{3.9}$$

where the non-negative terms have been eliminated.

Step 3: To control the terms containing $\hat{\boldsymbol{u}}_h^{n+1}$, by the definition of (3.7) we rewrite (3.4) as

$$\frac{\boldsymbol{u}_h^{n+1}-\hat{\boldsymbol{u}}_h^{n+1}}{\tau}+\frac{2}{3}\nabla_h(p_h^{n+1}-p_h^n)=0. \tag{3.10}$$

This in turn leads to

$$\|\hat{\boldsymbol{u}}_h^{n+1}\|_{L^2}^2=\|\boldsymbol{u}_h^{n+1}\|_{L^2}^2+\frac{4\tau^2}{9}\|\nabla_h(p_h^{n+1}-p_h^n)\|_{L^2}^2, \tag{3.11}$$

for which the equality $\big(\boldsymbol{u}_h^{n+1},\nabla_h(p_h^{n+1}-p_h^n)\big)=-\big(\nabla\cdot\boldsymbol{u}_h^{n+1},p_h^{n+1}-p_h^n\big)=0$ has been applied.

In addition, (3.10) is equivalent to

$$\frac{(2\boldsymbol{u}_h^{n+1}-\boldsymbol{u}_h^n)-(2\hat{\boldsymbol{u}}_h^{n+1}-\boldsymbol{u}_h^n)}{\tau}+\frac{4}{3}\nabla_h(p_h^{n+1}-p_h^n)=0,$$

which further implies

$$\|2\hat{\boldsymbol{u}}_h^{n+1}-\boldsymbol{u}_h^n\|_{L^2}^2=\|2\boldsymbol{u}_h^{n+1}-\boldsymbol{u}_h^n\|_{L^2}^2+\frac{16\tau^2}{9}\|\nabla_h(p_h^{n+1}-p_h^n)\|_{L^2}^2. \tag{3.12}$$

For the term $-\big(p_h^n,\nabla\cdot\hat{\boldsymbol{u}}_h^{n+1}\big)$, applying (3.10) again leads to

$$\begin{aligned}\big(\hat{\boldsymbol{u}}_h^{n+1},\nabla_h p_h^n\big)=&\big(\boldsymbol{u}_h^{n+1},\nabla_h p_h^n\big)+\big(\frac{2\tau}{3}\nabla_h(p_h^{n+1}-p_h^n),\nabla_h p_h^n\big)\\ =&\frac{\tau}{3}(\|\nabla_h p_h^{n+1}\|_{L^2}^2-\|\nabla_h p_h^n\|_{L^2}^2-\|\nabla_h(p_h^{n+1}-p_h^n)\|_{L^2}^2).\end{aligned} \tag{3.13}$$

Step 4: Substituting (3.11), (3.12) and (3.13) into (3.8) and (3.9), we obtain

$$\begin{aligned}&\frac{1}{4\tau}(\|\boldsymbol{H}_h^{n+1}\|_{L^2}^2-\|\boldsymbol{H}_h^n\|_{L^2}^2+\|2\boldsymbol{H}_h^{n+1}-\boldsymbol{H}_h^n\|_{L^2}^2-\|2\boldsymbol{H}_h^n-\boldsymbol{H}_h^{n-1}\|_{L^2}^2)\\ &+\frac{\mu_0}{4\tau}(\|\boldsymbol{u}_h^{n+1}\|_{L^2}^2+\frac{4\tau^2}{9}\|\nabla_h(p_h^{n+1}-p_h^n)\|_{L^2}^2-\|\boldsymbol{u}_h^n\|_{L^2}^2\\ &+\|2\boldsymbol{u}_h^{n+1}-\boldsymbol{u}_h^n\|_{L^2}^2+\frac{16\tau^2}{9}\|\nabla_h(p_h^{n+1}-p_h^n)\|_{L^2}^2-\|2\boldsymbol{u}_h^n-\boldsymbol{u}_h^{n-1}\|_{L^2}^2)\\ &+\frac{\mu_0\tau}{3}(\|\nabla_h p_h^{n+1}\|_{L^2}^2-\|\nabla_h p_h^n\|_{L^2}^2-\|\nabla_h(p_h^{n+1}-p_h^n)\|_{L^2}^2)+M^{n+1}(\frac{3M^{n+1}-4M^n+M^{n-1}}{2\tau})\\ &\leqslant 0,\end{aligned}$$

where we have used (3.6).

By the discrete energy function ε_h^n defined in Theorem 3.4, the energy stability follows immediately. The unconditional energy stability indicates that the corresponding homogeneous equations only admit trivial solutions, and this leads to the unique solvability immediately. This completes the proof of the theorem. □

3.3 Numerical implementation

In the practical implementation, we introduce more variables $\boldsymbol{H}_{ih}^{n+1}$,$\boldsymbol{\phi}_{ih}^{n+1}$ and $\hat{\boldsymbol{u}}_{ih}^{n+1}$, $i=1,2$, instead of computing $\boldsymbol{H}_h^{n+1}$, $\boldsymbol{\phi}_h^{n+1}$ and $\hat{\boldsymbol{u}}_h^{n+1}$ directly. $\boldsymbol{v}_{1h}$ is obtained by terms without M while $\boldsymbol{v}_{2h}$ is solved by terms containing M, $\boldsymbol{v}=\boldsymbol{H},\boldsymbol{\phi},\hat{\boldsymbol{u}}$. In specific, we write $\boldsymbol{H}_h^{n+1}$, $\boldsymbol{\phi}_h^{n+1}$ and $\hat{\boldsymbol{u}}_h^{n+1}$ as

$$\boldsymbol{H}_h^{n+1}=\boldsymbol{H}_{1h}^{n+1}+M^{n+1}\boldsymbol{H}_{2h}^{n+1},\quad \hat{\boldsymbol{u}}_h^{n+1}=\hat{\boldsymbol{u}}_{1h}^{n+1}+M^{n+1}\hat{\boldsymbol{u}}_{2h}^{n+1},\quad \boldsymbol{\phi}_h^{n+1}=\boldsymbol{\phi}_{1h}^{n+1}+M^{n+1}\boldsymbol{\phi}_{2h}^{n+1}\ , \tag{3.14}$$

and carry out the simulation of the discrete system (3.1)-(3.6) in the following four steps.

Step 1: By (3.14), we write (3.1) and (3.2) into the following equivalent forms

$$\begin{aligned} &\frac{3}{2\tau}\big(\boldsymbol{H}_{1h}^{n+1}, \boldsymbol{w}_h\big) + \frac{\eta}{\mu_0}\big(\nabla\times\boldsymbol{H}_{1h}^{n+1}, \nabla\times\boldsymbol{w}_h\big) + \frac{\eta}{\mu_0}\big(\nabla\cdot\boldsymbol{H}_{1h}^{n+1}, \nabla\cdot\boldsymbol{w}_h\big) \\ &\qquad + \frac{\eta_2}{\mu_0}\big(\nabla\times\boldsymbol{\phi}_{1h}^{n+1}, \nabla\times\boldsymbol{w}_h\big) + \frac{\eta_2}{\mu_0}\big(\nabla\cdot\boldsymbol{\phi}_{1h}^{n+1}, \nabla\cdot\boldsymbol{w}_h\big) = \frac{1}{2\tau}\big(4\boldsymbol{H}_h^n - \boldsymbol{H}_h^{n-1}, \boldsymbol{w}_h\big), \\ &\big(\nabla\times\boldsymbol{H}_{1h}^{n+1}, \nabla\times\boldsymbol{v}_h\big) + \big(\nabla\cdot\boldsymbol{H}_{1h}^{n+1}, \nabla\cdot\boldsymbol{v}_h\big) - \big(\boldsymbol{\phi}_{1h}^{n+1}, \boldsymbol{v}_h\big) = 0, \end{aligned} \tag{3.15}$$

and

$$\begin{aligned} &\frac{3}{2\tau}\big(\boldsymbol{H}_{2h}^{n+1}, \boldsymbol{w}_h\big) + \frac{\eta}{\mu_0}\big(\nabla\times\boldsymbol{H}_{2h}^{n+1}, \nabla\times\boldsymbol{w}_h\big) + \frac{\eta}{\mu_0}\big(\nabla\cdot\boldsymbol{H}_{2h}^{n+1}, \nabla\cdot\boldsymbol{w}_h\big) \\ &\qquad + \frac{\eta_2}{\mu_0}\big(\nabla\times\boldsymbol{\phi}_{2h}^{n+1}, \nabla\times\boldsymbol{w}_h\big) + \frac{\eta_2}{\mu_0}\big(\nabla\cdot\boldsymbol{\phi}_{2h}^{n+1}, \nabla\cdot\boldsymbol{w}_h\big) = \big(\tilde{\boldsymbol{u}}_h^{n+1}\times\widetilde{\boldsymbol{H}}_h^{n+1}, \nabla\times\boldsymbol{w}_h\big), \\ &\big(\nabla\times\boldsymbol{H}_{2h}^{n+1}, \nabla\times\boldsymbol{v}_h\big) + \big(\nabla\cdot\boldsymbol{H}_{2h}^{n+1}, \nabla\cdot\boldsymbol{v}_h\big) - \big(\boldsymbol{\phi}_{2h}^{n+1}, \boldsymbol{v}_h\big) = 0\ . \end{aligned} \tag{3.16}$$

Solving (3.15) and (3.16) gives $\boldsymbol{H}_{1h}^{n+1}$, $\boldsymbol{H}_{2h}^{n+1}$, $\boldsymbol{\phi}_{1h}^{n+1}$ and $\boldsymbol{\phi}_{2h}^{n+1}$.

Step 2: Again by (3.14), we could reformulate (3.3) as

$$\frac{3}{2\tau}\big(\hat{\boldsymbol{u}}_{1h}^{n+1}, \boldsymbol{l}_h\big) + \mu\big(\nabla\hat{\boldsymbol{u}}_{1h}^{n+1}, \nabla\boldsymbol{l}_h\big) = \frac{1}{2\tau}\big(4\boldsymbol{u}_h^n - \boldsymbol{u}_h^{n-1}, \boldsymbol{l}_h\big) + \big(p_h^n, \nabla\cdot\boldsymbol{l}_h\big)\ , \tag{3.17}$$

and

$$\frac{3}{2\tau}\big(\hat{\boldsymbol{u}}_{2h}^{n+1}, \boldsymbol{l}_h\big) + \mu\big(\nabla\hat{\boldsymbol{u}}_{2h}^{n+1}, \nabla\boldsymbol{l}_h\big) = -b\big(\tilde{\boldsymbol{u}}_h^{n+1}, \tilde{\boldsymbol{u}}_h^{n+1}, \boldsymbol{l}_h\big) - \frac{1}{\mu_0}\big(\widetilde{\boldsymbol{H}}_h^{n+1}\times(\nabla\times\widetilde{\boldsymbol{H}}_h^{n+1}), \boldsymbol{l}_h\big). \tag{3.18}$$

Then we get the values of $\hat{\boldsymbol{u}}_{1h}^{n+1}$ and $\hat{\boldsymbol{u}}_{2h}^{n+1}$ in this step.

Step 3: Substituting (3.14) into (3.6) leads to

$$\begin{aligned} \frac{3M^{n+1} - 4M^n + M^{n-1}}{2\tau} &= \big(\widetilde{\boldsymbol{H}}_h^{n+1}\times(\nabla\times\widetilde{\boldsymbol{H}}_h^{n+1}), \hat{\boldsymbol{u}}_{1h}^{n+1} + M^{n+1}\hat{\boldsymbol{u}}_{2h}^{n+1}\big) \\ &\quad + \mu_0 b\big(\tilde{\boldsymbol{u}}_h^{n+1}, \tilde{\boldsymbol{u}}_h^{n+1}, \hat{\boldsymbol{u}}_{1h}^{n+1} + M^{n+1}\hat{\boldsymbol{u}}_{2h}^{n+1}\big) \\ &\quad - \big(\tilde{\boldsymbol{u}}_h^{n+1}\times\widetilde{\boldsymbol{H}}_h^{n+1}, \nabla\times(\boldsymbol{H}_{1h}^{n+1} + M^{n+1}\boldsymbol{H}_{2h}^{n+1})\big) \\ &:= I_1 + M^{n+1}I_2. \end{aligned}$$

This in turn yields

$$M^{n+1} = \frac{2M^n - \frac{1}{2}M^{n-1} + \tau I_1}{\frac{3}{2} - \tau I_2}, \tag{3.19}$$

where we have already obtained all the values on the right hand side. Here, we denote

$$\begin{aligned} I_1 &= \big(\widetilde{\boldsymbol{H}}_h^{n+1}\times(\nabla\times\widetilde{\boldsymbol{H}}_h^{n+1}), \hat{\boldsymbol{u}}_{1h}^{n+1}\big) + \mu_0 b\big(\tilde{\boldsymbol{u}}_h^{n+1}, \tilde{\boldsymbol{u}}_h^{n+1}, \hat{\boldsymbol{u}}_{1h}^{n+1}\big) - \big(\tilde{\boldsymbol{u}}_h^{n+1}\times\widetilde{\boldsymbol{H}}_h^{n+1}, \nabla\times\boldsymbol{H}_{1h}^{n+1}\big), \\ I_2 &= \big(\widetilde{\boldsymbol{H}}_h^{n+1}\times(\nabla\times\widetilde{\boldsymbol{H}}_h^{n+1}), \hat{\boldsymbol{u}}_{2h}^{n+1}\big) + \mu_0 b\big(\tilde{\boldsymbol{u}}_h^{n+1}, \tilde{\boldsymbol{u}}_h^{n+1}, \hat{\boldsymbol{u}}_{2h}^{n+1}\big) - \big(\tilde{\boldsymbol{u}}_h^{n+1}\times\widetilde{\boldsymbol{H}}_h^{n+1}, \nabla\times\boldsymbol{H}_{2h}^{n+1}\big). \end{aligned}$$

Therefore, by adopting $\boldsymbol{w}_h = \boldsymbol{H}_{2h}^{n+1}, \boldsymbol{v}_h = \boldsymbol{\phi}_h^{n+1}$ in (3.16) and $\boldsymbol{l}_h = \hat{\boldsymbol{u}}_{2h}^{n+1}$ in (3.18), we have

$$\begin{aligned} -I_2 =& \frac{3}{2\tau}(\|\boldsymbol{H}_{2h}^{n+1}\|_{L^2}^2 + \mu_0\|\hat{\boldsymbol{u}}_{2h}^{n+1}\|_{L^2}^2) + \frac{\eta}{\mu_0}(\|\nabla\times\boldsymbol{H}_{2h}^{n+1}\|_{L^2}^2 + \|\nabla\cdot\boldsymbol{H}_{2h}^{n+1}\|_{L^2}^2) \\ &+ \frac{\eta_2}{\mu_0}\|\phi_{2h}^{n+1}\|_{L^2}^2 + \mu\mu_0\|\nabla\hat{\boldsymbol{u}}_{2h}^{n+1}\|_{L^2}^2 \geqslant 0, \end{aligned}$$

which guarantees that $\frac{3}{2} - \tau I_2 > 0$. As a conclusion, (3.19) is always solvable for M^{n+1}.

Step 4: Finally, $\boldsymbol{u}_h^{n+1}$ and p_h^{n+1} could be obtained by solving (3.4) and (3.5).

Remark 3.5. *It easy to see that by* (3.14)*, the whole system* (3.1)-(3.6) *consists of four separate sub-systems* (3.1)-(3.2)*,* (3.3)*,* (3.4)-(3.5) *and* (3.6)*. Therefore, solving the whole system together is exactly algebraically equivalent to solving it step by step as stated in subsection3.3. In the practical implementation,* Step 2 *generates an elliptic equation with constant coefficients, so that we could employ the conjugate gradient algorithm to solve it efficiently.* Step 3 *is just a direct algebraic calculation, and* Step 4 *corresponds to a Poisson-type equation. The main computational cost of the proposed scheme comes from* Step 1.

4 Optimal rate error estimate

We make the following regularity assumption for the solution of continuous system (1.1)-(1.3):

$$\begin{aligned}&\|\boldsymbol{H}_{ttt}\|_{L^\infty(0,T;L^2)} + \|\boldsymbol{H}_{tt}\|_{L^\infty(0,T;H^1)} + \|\boldsymbol{H}_t\|_{L^\infty(0,T;H^{r+1})} + \|\boldsymbol{H}\|_{L^\infty(0,T;H^{r+3})} + \|\boldsymbol{u}_{ttt}\|_{L^\infty(0,T;L^2)} \\ &+ \|\boldsymbol{u}_{tt}\|_{L^\infty(0,T;H^1)} + \|\boldsymbol{u}_t\|_{L^\infty(0,T;H^{r+1})} + \|\boldsymbol{u}\|_{L^\infty(0,T;H^{r+1})} + \|p_{tt}\|_{L^\infty(0,T;L^2)} + \|p_t\|_{L^\infty(0,T;H^{r+1})} \leqslant K\ . \end{aligned} \tag{4.1}$$

Here, v_t denotes the derivative of function v with respective to t. The optimal error estimate is stated in the following theorem.

Theorem 4.1. *Suppose that the classic solution* $(\boldsymbol{H}, \boldsymbol{u}, p)$ *to the equations* (1.1)-(1.3) *satisfies the regularity assumption* (4.1)*, and additionally* $\nabla p|_{\partial\Omega} = 0$*. Then there exist positive constants* τ_0 *and* h_0 *such that the numerical solution* $(\boldsymbol{H}_h^n, \boldsymbol{u}_h^n, p_h^n), 2 \leqslant n \leqslant N$*, obtained from the scheme* (3.1)-(3.6) *satisfies, as* $\tau < \tau_0$*,* $h < h_0$ *and* $\tau = \mathcal{O}(h)$*,*

$$\max_{2\leqslant n\leqslant N}(\|\boldsymbol{H}_h^n - \boldsymbol{H}^n\|_{L^2} + \|\boldsymbol{u}_h^n - \boldsymbol{u}^n\|_{L^2}) \leqslant C_0(\tau^2 + h^{r+1}), \tag{4.2}$$

where C_0 *is a positive constant independent of* τ *and* h*.*

4.1 Projections

We first introduce in this subsection several types of projections and their properties. For $v \in L^2(\Omega)$ (or $\boldsymbol{v} \in \boldsymbol{L}^2(\Omega)$), we denote by P_h the L^2 projection as

$$(v - P_h v, q_h) = 0,\ \forall q_h \in Q_h \text{ (or } (\boldsymbol{v} - P_h\boldsymbol{v}, \boldsymbol{q}_h) = 0,\ \forall \boldsymbol{q}_h \in \mathbf{X}_h). \tag{4.3}$$

For $(\boldsymbol{u}, p) \in \mathbf{H}_0^1(\Omega) \times L^2(\Omega)/\mathbb{R}$, let $(\boldsymbol{R}_h\boldsymbol{u}, R_h p)$ denote the Stokes projection

$$\mu(\nabla(\boldsymbol{u} - \boldsymbol{R}_h\boldsymbol{u}), \nabla\boldsymbol{v}_h) - (p - R_h p, \nabla\cdot\boldsymbol{v}_h) = 0, \qquad \forall\, \boldsymbol{v}_h \in \mathbf{X}_h, \tag{4.4}$$

$$(\nabla\cdot(\boldsymbol{u} - \boldsymbol{R}_h\boldsymbol{u}), q_h) = 0, \qquad \forall\, q_h \in Q_h. \tag{4.5}$$

For $\boldsymbol{H} \in \mathring{\mathbf{H}}^1(\Omega)$, the Maxwell projection is given by

$$(\nabla\times(\boldsymbol{H} - \Pi_h\boldsymbol{H}), \nabla\times\boldsymbol{w}_h) + (\nabla\cdot(\boldsymbol{H} - \Pi_h\boldsymbol{H}), \nabla\cdot\boldsymbol{w}_h) = 0, \quad \forall \boldsymbol{w}_h \in \mathbf{S}_h. \tag{4.6}$$

We present the results on the estimates of these projections, and the corresponding proofs are referred to [21] and [44].

Lemma 4.2. *We have the following inequalities: For* $m = 0, 1,\ 0 \leqslant \ell \leqslant r,\ 1 \leqslant s \leqslant \infty$*,*

$$\|P_h v\|_{W^{m,s}} \leqslant C\|v\|_{W^{m,s}}, \tag{4.7}$$

$$\|v - P_h v\|_{L^2} \leqslant Ch^{\ell+1}\|v\|_{H^{\ell+1}}. \tag{4.8}$$

For $0 \leqslant \ell \leqslant r$, $1 < s < \infty$,

$$\|\boldsymbol{R}_h \boldsymbol{u}\|_{W^{1,s}} + \|R_h p\|_{L^s} \leqslant C(\|\boldsymbol{u}\|_{W^{1,s}} + \|p\|_{L^s}), \tag{4.9}$$

$$\|\boldsymbol{u} - \boldsymbol{R}_h \boldsymbol{u}\|_{L^s} + h\|\boldsymbol{u} - \boldsymbol{R}_h \boldsymbol{u}\|_{W^{1,s}} \leqslant Ch^{\ell+1}(\|\boldsymbol{u}\|_{W^{\ell+1,s}} + \|p\|_{W^{\ell,s}}), \tag{4.10}$$

$$\|p - R_h p\|_{L^s} \leqslant Ch^{\ell}(\|\boldsymbol{u}\|_{W^{\ell+1,s}} + \|p\|_{W^{\ell,s}}), \tag{4.11}$$

$$\|\partial_t(\boldsymbol{u} - \boldsymbol{R}_h \boldsymbol{u})\|_{L^s} + h\|\partial_t(p - R_h p)\|_{L^s} \leqslant Ch^{\ell+1}(\|\partial_t \boldsymbol{u}\|_{W^{\ell+1,s}} + \|\partial_t p\|_{W^{\ell,s}}). \tag{4.12}$$

For $0 \leqslant \ell \leqslant r$,

$$\|\boldsymbol{H} - \Pi_h \boldsymbol{H}\|_{L^2} + h\|\boldsymbol{H} - \Pi_h \boldsymbol{H}\|_{H^1} \leqslant Ch^{\ell+1}\|\boldsymbol{H}\|_{H^{\ell+1}}. \tag{4.13}$$

All constants C *in the above inequalities are positive and independent of* h.

Moreover, we need the following inverse inequality ([4]).

Lemma 4.3. *For* $\forall\, v_h \in Q_h$, $\mathbf{X}_h$ *or* $\mathbf{S}_h$, *it holds that*

$$\|v_h\|_{W^{m,s}} \leqslant Ch^{n-m+\frac{d}{s}-\frac{d}{q}}\|v_h\|_{W^{n,q}}, \tag{4.14}$$

for $0 \leqslant n \leqslant m \leqslant 1$, $1 \leqslant q \leqslant s \leqslant \infty$, *where* d *is the dimension of the space, and* C *is a positive constant independent of* h.

In addition, we give an estimate of the discrete gradient operator ∇_h defined in (3.7).

Lemma 4.4. *For* $\forall\, q_h \in Q_h$, *we have*

$$\|\nabla_h q_h\|_{L^2} \leqslant Ch^{-1}\|q_h\|_{L^2}, \tag{4.15}$$

where C *is a positive constant independent of* h.

Proof. Taking $\boldsymbol{v}_h = \nabla_h q_h$ in (3.7) gives

$$\|\nabla_h q_h\|_{L^2}^2 = (-\nabla \cdot \nabla_h q_h, q_h) \leqslant \|\nabla \cdot \nabla_h q_h\|_{L^2} \cdot \|q_h\|_{L^2} \leqslant Ch^{-1}\|\nabla_h q_h\|_{L^2} \cdot \|q_h\|_{L^2},$$

where the Hölder inequality and inverse inequality (4.14) have been used. The proof is completed by eliminating the term $\|\nabla_h q_h\|_{L^2}$ on both sides of the above inequality.

□

4.2 Error equations

To tackle the term $\hat{\boldsymbol{u}}_h^{n+1}$, we introduce an intermediate function $\widehat{\boldsymbol{R}_h \boldsymbol{u}^{n+1}} \in \mathbf{X}_h$ satisfying

$$\frac{\boldsymbol{R}_h \boldsymbol{u}^{n+1} - \widehat{\boldsymbol{R}_h \boldsymbol{u}^{n+1}}}{\tau} + \frac{2}{3}\nabla_h(R_h p^{n+1} - R_h p^n) = 0. \tag{4.16}$$

With the above function and the projections defined in the previous subsection, we could rewrite (2.1) and (2.4)-(2.7) as

$$\begin{aligned}
&\big(\frac{3\Pi_h\boldsymbol{H}^{n+1}-4\Pi_h\boldsymbol{H}^{n}+\Pi_h\boldsymbol{H}^{n-1}}{2\tau},\boldsymbol{w}_h\big)-M_e^{n+1}\big(\tilde{\boldsymbol{u}}^{n+1}\times\widetilde{\boldsymbol{H}}^{n+1},\nabla\times\boldsymbol{w}_h\big)\\
&\quad+\frac{\eta}{\mu_0}\big(\nabla\times\Pi_h\boldsymbol{H}^{n+1},\nabla\times\boldsymbol{w}_h\big)+\frac{\eta}{\mu_0}\big(\nabla\cdot\Pi_h\boldsymbol{H}^{n+1},\nabla\cdot\boldsymbol{w}_h\big)\\
&\quad+\frac{\eta_2}{\mu_0}\big(\nabla\times\Pi_h\boldsymbol{\phi}^{n+1},\nabla\times\boldsymbol{w}_h\big)+\frac{\eta_2}{\mu_0}\big(\nabla\cdot\Pi_h\boldsymbol{\phi}^{n+1},\nabla\cdot\boldsymbol{w}_h\big)=\mathcal{T}_{\boldsymbol{H}}^{n+1}(\boldsymbol{w}_h), &(4.17)\\
&\Big(\nabla\times\Pi_h\boldsymbol{H}^{n+1},\nabla\times\boldsymbol{v}_h\Big)+\Big(\nabla\cdot\Pi_h\boldsymbol{H}^{n+1},\nabla\cdot\boldsymbol{v}_h\Big)-\big(\Pi_h\boldsymbol{\phi}^{n+1},\boldsymbol{v}_h\big)=\mathcal{T}_{\boldsymbol{\phi}}^{n+1}(\boldsymbol{w}_h), &(4.18)\\
&\big(\frac{3\widehat{\boldsymbol{R}_h\boldsymbol{u}^{n+1}}-4\boldsymbol{R}_h\boldsymbol{u}^{n}+\boldsymbol{R}_h\boldsymbol{u}^{n-1}}{2\tau},\boldsymbol{l}_h\big)+\mu\big(\nabla\widehat{\boldsymbol{R}_h\boldsymbol{u}^{n+1}},\nabla\boldsymbol{l}_h\big)+M_e^{n+1}b\big(\tilde{\boldsymbol{u}}^{n+1},\tilde{\boldsymbol{u}}^{n+1},\boldsymbol{l}_h\big)\\
&\quad-\big(R_hp^n,\nabla\cdot\boldsymbol{l}_h\big)+\frac{M_e^{n+1}}{\mu_0}\big(\widetilde{\boldsymbol{H}}^{n+1}\times(\nabla\times\widetilde{\boldsymbol{H}}^{n+1}),\boldsymbol{l}_h\big)=\frac{3}{2}\big(\frac{\widehat{\boldsymbol{R}_h\boldsymbol{u}^{n+1}}-\boldsymbol{R}_h\boldsymbol{u}^{n+1}}{\tau},\boldsymbol{l}_h\big)\\
&\quad+\mu\big(\nabla(\widehat{\boldsymbol{R}_h\boldsymbol{u}^{n+1}}-\boldsymbol{R}_h\boldsymbol{u}^{n+1}),\nabla\boldsymbol{l}_h\big)-\big(R_h(p^n-p^{n+1}),\nabla\cdot\boldsymbol{l}_h\big)+\mathcal{T}_{\boldsymbol{u}}^{n+1}(\boldsymbol{l}_h), &(4.19)\\
&\big(\nabla\cdot\boldsymbol{R}_h\boldsymbol{u}^{n+1},q_h\big)=0, &(4.20)\\
&\frac{3M_e^{n+1}-4M_e^{n}+M_e^{n-1}}{2\tau}=\mu_0b(\tilde{\boldsymbol{u}}^{n+1},\tilde{\boldsymbol{u}}^{n+1},\boldsymbol{u}^{n+1})+\big(\widetilde{\boldsymbol{H}}^{n+1}\times(\nabla\times\widetilde{\boldsymbol{H}}^{n+1}),\boldsymbol{u}^{n+1}\big)\\
&\quad-\big(\tilde{\boldsymbol{u}}^{n+1}\times\widetilde{\boldsymbol{H}}^{n+1},\nabla\times\boldsymbol{H}^{n+1}\big)+\mathcal{T}_M, &(4.21)
\end{aligned}$$

for any $(\boldsymbol{w}_h,\boldsymbol{v}_h,\boldsymbol{l}_h,q_h)\in(\mathring{\mathbf{H}}^1(\Omega),\mathring{\mathbf{H}}^1(\Omega),\mathbf{H}_0^1(\Omega),L^2(\Omega))$, where we have introduced an artificial variable $\hat{\boldsymbol{u}}^{n+1}:=\boldsymbol{u}^{n+1}$, and have combined (3.3) with (3.4) to obtain (4.19). Here, the truncation errors $\mathcal{T}_{\boldsymbol{H}}^{n+1}$, $\mathcal{T}_{\boldsymbol{\phi}}^{n+1}$, $\mathcal{T}_{\boldsymbol{u}}^{n+1}$ and $\mathcal{T}_M^{n+1}$ are given by

$$\begin{aligned}
\mathcal{T}_{\boldsymbol{H}}^{n+1}(\boldsymbol{w}_h)=&\big(\frac{3\Pi_h\boldsymbol{H}^{n+1}-4\Pi_h\boldsymbol{H}^{n}+\Pi_h\boldsymbol{H}^{n-1}}{2\tau}-\partial_t\boldsymbol{H}^{n+1},\boldsymbol{w}_h\big)\\
&-M_e^{n+1}\big(\boldsymbol{u}^{n+1}\times\boldsymbol{H}^{n+1}-\tilde{\boldsymbol{u}}^{n+1}\times\widetilde{\boldsymbol{H}}^{n+1},\nabla\times\boldsymbol{w}_h\big),\\
\mathcal{T}_{\boldsymbol{\phi}}^{n+1}(\boldsymbol{v}_h)=&-\big(\Pi_h\boldsymbol{\phi}^{n+1}-\boldsymbol{\phi}^{n+1},\boldsymbol{v}_h\big),\\
\mathcal{T}_{\boldsymbol{u}}^{n+1}(\boldsymbol{l}_h)=&\big(\frac{3\boldsymbol{R}_h\boldsymbol{u}^{n+1}-4\boldsymbol{R}_h\boldsymbol{u}^{n}+\boldsymbol{R}_h\boldsymbol{u}^{n-1}}{2\tau}-\partial_t\boldsymbol{u}^{n+1},\boldsymbol{l}_h\big)\\
&+M_e^{n+1}(b(\tilde{\boldsymbol{u}}^{n+1},\tilde{\boldsymbol{u}}^{n+1},\boldsymbol{l}_h)-b(\boldsymbol{u}^{n+1},\boldsymbol{u}^{n+1},\boldsymbol{l}_h))\\
&+\frac{M_e^{n+1}}{\mu_0}\big(\widetilde{\boldsymbol{H}}^{n+1}\times(\nabla\times\widetilde{\boldsymbol{H}}^{n+1})-\boldsymbol{H}^{n+1}\times(\nabla\times\boldsymbol{H}^{n+1}),\boldsymbol{l}_h\big),\\
\mathcal{T}_M=&\big[\frac{3M_e^{n+1}-4M_e^{n}+M_e^{n-1}}{2\tau}-M_t^{n+1}\big]+\mu_0\big[b(\boldsymbol{u}^{n+1},\boldsymbol{u}^{n+1},\boldsymbol{u}^{n+1})-b(\tilde{\boldsymbol{u}}^{n+1},\tilde{\boldsymbol{u}}^{n+1},\boldsymbol{u}^{n+1})\big]\\
&+\big[\big(\boldsymbol{H}^{n+1}\times(\nabla\times\boldsymbol{H}^{n+1}),\boldsymbol{u}^{n+1}\big)-\big(\widetilde{\boldsymbol{H}}^{n+1}\times(\nabla\times\widetilde{\boldsymbol{H}}^{n+1}),\boldsymbol{u}^{n+1}\big)\big]\\
&-\big[\big(\boldsymbol{u}^{n+1}\times\boldsymbol{H}^{n+1},\nabla\times\boldsymbol{H}^{n+1}\big)-\big(\tilde{\boldsymbol{u}}^{n+1}\times\widetilde{\boldsymbol{H}}^{n+1},\nabla\times\boldsymbol{H}^{n+1}\big)\big].
\end{aligned}$$

Since the projection error estimates have been given in Lemma 4.2, we only need to analyze the errors generated by the following error functions, for $n=1,2,...N$,

$$\begin{aligned}
&e_{\boldsymbol{H}}^n=\Pi_h\boldsymbol{H}^n-\boldsymbol{H}_h^n,\quad e_{\boldsymbol{\phi}}^n=\Pi_h\boldsymbol{\phi}^n-\boldsymbol{\phi}_h^n,\\
&e_{\boldsymbol{u}}^n=\boldsymbol{R}_h\boldsymbol{u}^n-\boldsymbol{u}_h^n,\quad \hat{e}_{\boldsymbol{u}}^n=\widehat{\boldsymbol{R}_h\boldsymbol{u}^n}-\hat{\boldsymbol{u}}_h^n\ ,\quad e_p^n=R_hp^n-p_h^n\ .
\end{aligned}$$

Subtracting the numerical scheme (3.1)-(3.5) from the projection system (4.17)-(4.20), and applying

(4.16), we have

$$
\begin{aligned}
&\Big(\frac{3e_{\boldsymbol{H}}^{n+1}-4e_{\boldsymbol{H}}^{n}+e_{\boldsymbol{H}}^{n-1}}{2\tau},\boldsymbol{w}_h\Big)-\big[M_e^{n+1}\big(\widetilde{\boldsymbol{u}}^{n+1}\times\widetilde{\boldsymbol{H}}^{n+1},\nabla\times\boldsymbol{w}_h\big)-M^{n+1}\big(\widetilde{\boldsymbol{u}}_h^{n+1}\times\widetilde{\boldsymbol{H}}_h^{n+1},\nabla\times\boldsymbol{w}_h\big)\big]\\
&\qquad+\frac{\eta}{\mu_0}\big(\nabla\times e_{\boldsymbol{H}}^{n+1},\nabla\times\boldsymbol{w}_h\big)+\frac{\eta}{\mu_0}\big(\nabla\cdot e_{\boldsymbol{H}}^{n+1},\nabla\cdot\boldsymbol{w}_h\big)\\
&\qquad+\frac{\eta_2}{\mu_0}\big(\nabla\times e_{\boldsymbol{\phi}}^{n+1},\nabla\times\boldsymbol{w}_h\big)+\frac{\eta_2}{\mu_0}\big(\nabla\cdot e_{\boldsymbol{\phi}}^{n+1},\nabla\cdot\boldsymbol{w}_h\big)=\mathcal{T}_{\boldsymbol{H}}^{n+1}(\boldsymbol{w}_h), && (4.22)\\
&\big(\nabla\times e_{\boldsymbol{H}}^{n+1},\nabla\times\boldsymbol{v}_h\big)+\big(\nabla\cdot e_{\boldsymbol{H}}^{n+1},\nabla\cdot\boldsymbol{v}_h\big)-\big(e_{\boldsymbol{\phi}}^{n+1},\boldsymbol{v}_h\big)=\mathcal{T}_{\boldsymbol{\phi}}^{n+1}(\boldsymbol{v}_h), && (4.23)\\
&\Big(\frac{3\hat{e}_{\boldsymbol{u}}^{n+1}-4e_{\boldsymbol{u}}^{n}+e_{\boldsymbol{u}}^{n-1}}{2\tau},\boldsymbol{l}_h\Big)+\mu\big(\nabla\hat{e}_{\boldsymbol{u}}^{n+1},\nabla\boldsymbol{l}_h\big)+\big(M_e^{n+1}b(\widetilde{\boldsymbol{u}}^{n+1},\widetilde{\boldsymbol{u}}^{n+1},\boldsymbol{l}_h)-M^{n+1}b(\widetilde{\boldsymbol{u}}_h^{n+1},\widetilde{\boldsymbol{u}}_h^{n+1},\boldsymbol{l}_h)\big)\\
&\qquad-\big(e_p^n,\nabla\cdot\boldsymbol{l}_h\big)+\frac{1}{\mu_0}\big[M_e^{n+1}\big(\widetilde{\boldsymbol{H}}^{n+1}\times(\nabla\times\widetilde{\boldsymbol{H}}^{n+1}),\boldsymbol{l}_h\big)-M^{n+1}\big(\widetilde{\boldsymbol{H}}_h^{n+1}\times(\nabla\times\widetilde{\boldsymbol{H}}_h^{n+1}),\boldsymbol{l}_h\big)\big]\\
&\quad=\frac{3}{2\tau}\big(\widehat{\boldsymbol{R}_h\boldsymbol{u}^{n+1}}-\boldsymbol{R}_h\boldsymbol{u}^{n+1},\boldsymbol{l}_h\big)+\mu\big(\nabla(\widehat{\boldsymbol{R}_h\boldsymbol{u}^{n+1}}-\boldsymbol{R}_h\boldsymbol{u}^{n+1}),\nabla\boldsymbol{l}_h\big)-\big(R_hp^n-R_hp^{n+1},\nabla\cdot\boldsymbol{l}_h\big)\\
&\qquad+\mathcal{T}_{\boldsymbol{u}}^{n+1}(\boldsymbol{l}_h), && (4.24)\\
&\Big(\frac{e_{\boldsymbol{u}}^{n+1}-\hat{e}_{\boldsymbol{u}}^{n+1}}{\tau},\boldsymbol{r}_h\Big)-\frac{2}{3}\big(e_p^{n+1}-e_p^n,\nabla\cdot\boldsymbol{r}_h\big)=0, && (4.25)\\
&\big(\nabla\cdot e_{\boldsymbol{u}}^{n+1},q_h\big)=0, && (4.26)
\end{aligned}
$$

for any $(\boldsymbol{w}_h,\boldsymbol{v}_h,\boldsymbol{l}_h,\boldsymbol{r}_h,q_h)\in(\mathbf{S}_h,\mathbf{S}_h,\mathbf{X}_h,\mathbf{X}_h,Q_h)$, and $n=1,2,...N-1$.

4.3 Proof of Theorem 4.1

We give the following estimates needed in the later proof.

Lemma 4.5. *Under the regularity assumption* (4.1)*, the following are valid that*

$$\|\nabla_h P_h\partial_t p-P_h\nabla\partial_t p\|_{L^2}\leqslant Ch, \tag{4.27}$$

$$\|\nabla_h(R_hp^{n+1}-R_hp^n)\|_{L^2}\leqslant C\tau, \tag{4.28}$$

where C is a positive constant independent of h and τ.

Proof. For $\boldsymbol{v}_h\in\mathbf{X}_h$, we have

$$
\begin{aligned}
&\big(\nabla_hP_h\partial_tp-P_h\nabla\partial_tp,\boldsymbol{v}_h\big)\\
=&\big(\nabla_hP_h\partial_tp-\nabla\partial_tp,\boldsymbol{v}_h\big)\\
=&-\big(P_h\partial_tp-\partial_tp,\nabla\cdot\boldsymbol{v}_h\big)\\
\leqslant&\|P_h\partial_tp-\partial_tp\|_{L^2}\|\nabla\cdot\boldsymbol{v}_h\|_{L^2}\quad\text{(by (4.8) and (4.14))}\\
\leqslant&Ch^2\cdot Ch^{-1}\|\boldsymbol{v}_h\|_{L^2}=Ch\|\boldsymbol{v}_h\|_{L^2}.
\end{aligned}
$$

Consequently, using the duality of $L^2(\Omega)$ itself gives (4.27).

For (4.28), we see that

$$
\begin{aligned}
&\|\nabla_h(R_hp^{n+1}-R_hp^n)\|_{L^2}\\
=&C\tau\|\nabla_hR_h\partial_tp\|_{L^2}+C\tau^2\quad\text{(by Taylor expansions and p for p^{n+1} in short)}\\
\leqslant&C\tau\big(\|\nabla_hR_h\partial_tp-\nabla_hP_h\partial_tp\|_{L^2}+\|\nabla_hP_h\partial_tp-\nabla P_h\partial_tp\|_{L^2}+\|\nabla P_h\partial_tp\|_{L^2}\big)+C\tau^2\\
\leqslant&C\tau\big(Ch^{-1}(\|R_h\partial_tp-\partial_tp\|_{L^2}+\|\partial_tp-P_h\partial_tp\|_{L^2})+Ch+C\big)+C\tau^2\quad\text{(by (4.15), (4.27) and (4.7))}\\
\leqslant&C\tau\big(Ch^{-1}h^2+C\big)+C\tau^2\quad\text{(by (4.12) and (4.8))}\\
\leqslant&C\tau,
\end{aligned}
$$

where the regularity assumption (4.1) has been used frequently. This completes the proof. □

We will establish the error estimates by using the mathematical induction, and then make the assumption at the previous time step that

$$\|e_{\boldsymbol{H}}^m\|_{L^2} + \|e_{\boldsymbol{u}}^m\|_{L^2} \leqslant h^{\frac{9}{5}} + \tau^{\frac{9}{5}}, \quad \text{for } m \leqslant n. \tag{4.29}$$

This induction will be recovered at the next step t^{n+1}, as will be demonstrated later. Remark 3.3 indicates that the induction assumption (4.29) is valid for $m = 0, 1$, and then for $m \leqslant n$ we have

$$\begin{aligned}
\|\boldsymbol{u}_h^m\|_{L^\infty} \leqslant & C\|\boldsymbol{u}_h^m\|_{W^{1,4}} \\
\leqslant & C(\|e_{\boldsymbol{u}}^m\|_{W^{1,4}} + \|\boldsymbol{R}_h\boldsymbol{u}^m - \boldsymbol{u}^m\|_{W^{1,4}} + \|\boldsymbol{u}^m\|_{W^{1,4}}) \\
\leqslant & Ch^{-\frac{d}{4}-1}(\|\boldsymbol{u}_h^m - \boldsymbol{R}_h\boldsymbol{u}^m\|_{L^2}) + C\|\boldsymbol{R}_h\boldsymbol{u}^m - \boldsymbol{u}^m\|_{W^{1,4}} + \|\boldsymbol{u}^m\|_{L^\infty} \quad \text{(by (4.14))} \\
\leqslant & Ch^{-\frac{d}{4}-1}(h^{\frac{9}{5}} + \tau^{\frac{9}{5}} + h^2) + K \quad \text{(by (4.29) and (4.10))} \\
\leqslant & K^*,
\end{aligned} \tag{4.30}$$

and

$$\begin{aligned}
\|\boldsymbol{H}_h^m\|_{L^\infty} & \leqslant C\|\boldsymbol{H}_h^m\|_{W^{1,4}} \\
& \leqslant C(\|e_{\boldsymbol{H}}^m\|_{W^{1,4}} + \|\Pi_h\boldsymbol{H}^m - I_h\boldsymbol{H}^m\|_{W^{1,4}} + \|I_h\boldsymbol{H}^m\|_{W^{1,4}}) \\
& \leqslant Ch^{-\frac{d}{4}-1}\|e_{\boldsymbol{H}}^m\|_{L^2} + Ch^{-\frac{d}{4}}\|\Pi_h\boldsymbol{H}^m - I_h\boldsymbol{H}^m\|_{H^1} + C\|I_h\boldsymbol{H}^m\|_{W^{1,4}} \quad \text{(by (4.14))} \\
& \leqslant Ch^{\frac{4}{5}-\frac{d}{4}} + Ch^{-\frac{d}{4}}(\|\Pi_h\boldsymbol{H}^m - \boldsymbol{H}^m\|_{H^1} + \|I_h\boldsymbol{H}^m - \boldsymbol{H}^m\|_{H^1}) + CK \quad \text{(by (4.29))} \\
& \leqslant CK + Ch^{-\frac{d}{4}}(h^2 + h^2) \quad \text{(by (4.13))} \\
& \leqslant K^*,
\end{aligned} \tag{4.31}$$

where I_h denotes the standard Lagrange interpolation, and we have utilized its stability and error estimates from [14] in the last second inequality. Also, we have used the Sobolev inequality twice to control the L^∞-norm by $W^{1,4}$-norm.

Thus we obtain the bound of the numerical solutions

$$\|\boldsymbol{H}_h^m\|_{L^\infty} + \|\boldsymbol{u}_h^m\|_{L^\infty} \leqslant K^*, \quad m \leqslant n. \tag{4.32}$$

Now we proceed with the proof of Theorem 4.1.

Proof. Step 1: Taking $\boldsymbol{w}_h = e_{\boldsymbol{H}}^{n+1}$ in (4.22) and $\boldsymbol{v}_h = e_{\boldsymbol{\phi}}^{n+1}$ in (4.23), we have

$$\begin{aligned}
& \frac{1}{4\tau}(\|e_{\boldsymbol{H}}^{n+1}\|_{L^2}^2 - \|e_{\boldsymbol{H}}^n\|_{L^2}^2 + \|2e_{\boldsymbol{H}}^{n+1} - e_{\boldsymbol{H}}^n\|_{L^2}^2 - \|2e_{\boldsymbol{H}}^n - e_{\boldsymbol{H}}^{n-1}\|_{L^2}^2) \\
& + \frac{\eta}{\mu_0}(\|\nabla \times e_{\boldsymbol{H}}^{n+1}\|_{L^2}^2 + \|\nabla \cdot e_{\boldsymbol{H}}^{n+1}\|_{L^2}^2) + \frac{\eta_2}{\mu_0}\|e_{\boldsymbol{\phi}}^{n+1}\|_{L^2}^2 \\
= & \big[M_e^{n+1}\big(\widetilde{\boldsymbol{u}}^{n+1} \times \widetilde{\boldsymbol{H}}^{n+1}, \nabla \times e_{\boldsymbol{H}}^{n+1}\big) - M^{n+1}\big(\widetilde{\boldsymbol{u}}_h^{n+1} \times \widetilde{\boldsymbol{H}}_h^{n+1}, \nabla \times e_{\boldsymbol{H}}^{n+1}\big)\big] \\
& + \mathcal{T}_{\boldsymbol{H}}^{n+1}(e_{\boldsymbol{H}}^{n+1}) - \frac{\eta_2}{\mu_0}\mathcal{T}_{\boldsymbol{\phi}}^{n+1}(e_{\boldsymbol{\phi}}^{n+1}) := \sum_{i=1}^{3} I_{1,i}.
\end{aligned} \tag{4.33}$$

The nonlinear terms $I_{1,1}$ could be analyzed as follows, due to the fact that $M_e \equiv 1$,

$$\begin{aligned}
I_{1,1} =& \big(\widetilde{\boldsymbol{u}}^{n+1} \times (\widetilde{\boldsymbol{H}}^{n+1} - \Pi_h \widetilde{\boldsymbol{H}}^{n+1}), \nabla \times e_{\boldsymbol{H}}^{n+1}\big) + \big(\widetilde{\boldsymbol{u}}^{n+1} \times \tilde{e}_{\boldsymbol{H}}^{n+1}, \nabla \times e_{\boldsymbol{H}}^{n+1}\big) \\
&+ \big((\widetilde{\boldsymbol{u}}^{n+1} - \boldsymbol{R}_h \widetilde{\boldsymbol{u}}^{n+1}) \times \widetilde{\boldsymbol{H}}_h^{n+1}, \nabla \times e_{\boldsymbol{H}}^{n+1}\big) + \big(\tilde{e}_{\boldsymbol{u}}^{n+1} \times \widetilde{\boldsymbol{H}}_h^{n+1}, \nabla \times e_{\boldsymbol{H}}^{n+1}\big) \\
&+ (M_e^{n+1} - M^{n+1})\big(\widetilde{\boldsymbol{u}}_h^{n+1} \times \widetilde{\boldsymbol{H}}_h^{n+1}, \nabla \times e_{\boldsymbol{H}}^{n+1}\big) \\
\leqslant& \|\widetilde{\boldsymbol{u}}^{n+1}\|_{L^\infty} \|\widetilde{\boldsymbol{H}}^{n+1} - \Pi_h \widetilde{\boldsymbol{H}}^{n+1}\|_{L^2} \|\nabla \times e_{\boldsymbol{H}}^{n+1}\|_{L^2}^2 + \|\widetilde{\boldsymbol{u}}^{n+1}\|_{L^\infty} \|\tilde{e}_{\boldsymbol{H}}^{n+1}\|_{L^2} \|\nabla \times e_{\boldsymbol{H}}^{n+1}\|_{L^2} \\
&+ \|\widetilde{\boldsymbol{u}}^{n+1} - \boldsymbol{R}_h \widetilde{\boldsymbol{u}}^{n+1}\|_{L^2} \|\widetilde{\boldsymbol{H}}_h^{n+1}\|_{L^\infty} \|\nabla \times e_{\boldsymbol{H}}^{n+1}\|_{L^2} + \|\tilde{e}_{\boldsymbol{u}}^{n+1}\|_{L^2} \|\widetilde{\boldsymbol{H}}_h^{n+1}\|_{L^\infty} \|\nabla \times e_{\boldsymbol{H}}^{n+1}\|_{L^2} \\
&+ |M_e^{n+1} - M^{n+1}| \|\widetilde{\boldsymbol{u}}_h^{n+1}\|_{L^\infty} \|\widetilde{\boldsymbol{H}}_h^{n+1}\|_{L^2} \|\nabla \times e_{\boldsymbol{H}}^{n+1}\|_{L^2} \\
\leqslant& C(h^{2r+2} + \|\tilde{e}_{\boldsymbol{H}}^{n+1}\|_{L^2}^2 + \|\tilde{e}_{\boldsymbol{u}}^{n+1}\|_{L^2}^2 + (M_e^{n+1} - M^{n+1})^2) + \frac{\eta}{4\mu_0} \|\nabla \times e_{\boldsymbol{H}}^{n+1}\|_{L^2}^2, \qquad (4.34)
\end{aligned}$$

where we have utilized the regularity assumption (4.1), the bound of numerical solutions (4.32), the Cauchy inequality and the Hölder inequality.

The truncation error terms could be bounded as

$$I_{1,2} \leqslant C(h^{2r+2} + \tau^4 + \|e_{\boldsymbol{H}}^{n+1}\|_{L^2}^2) + \frac{\eta}{4\mu_0} \|\nabla \times e_{\boldsymbol{H}}^{n+1}\|_{L^2}^2, \qquad (4.35)$$

and

$$I_{1,3} = \frac{\eta_2}{\mu_0}\big(\Pi_h \boldsymbol{\phi}^{n+1} - \boldsymbol{\phi}^{n+1}, e_{\boldsymbol{\phi}}^{n+1}\big) \leqslant Ch^{2r+2} + \frac{\eta_2}{2\mu_0} \|e_{\boldsymbol{\phi}}^{n+1}\|_{L^2}^2. \qquad (4.36)$$

where the Cauchy inequality and the projection estimate (4.13) have been used.

Thus by using (4.34), (4.35) and (4.36), (4.33) could be rewritten as

$$\begin{aligned}
&\frac{1}{4\tau}(\|e_{\boldsymbol{H}}^{n+1}\|_{L^2}^2 - \|e_{\boldsymbol{H}}^{n}\|_{L^2}^2 + \|2e_{\boldsymbol{H}}^{n+1} - e_{\boldsymbol{H}}^{n}\|_{L^2}^2 - \|2e_{\boldsymbol{H}}^{n} - e_{\boldsymbol{H}}^{n-1}\|_{L^2}^2) \\
&+ \frac{\eta}{2\mu_0} \|\nabla \times e_{\boldsymbol{H}}^{n+1}\|_{L^2}^2 + \frac{\eta}{\mu_0} \|\nabla \cdot e_{\boldsymbol{H}}^{n+1}\|_{L^2}^2 + \frac{\eta_2}{2\mu_0} \|e_{\boldsymbol{\phi}}^{n+1}\|_{L^2}^2 \\
\leqslant& C[h^{2r+2} + \tau^4 + \|\tilde{e}_{\boldsymbol{H}}^{n+1}\|_{L^2}^2 + \|\tilde{e}_{\boldsymbol{u}}^{n+1}\|_{L^2}^2 + (M_e^{n+1} - M^{n+1})^2]. \qquad (4.37)
\end{aligned}$$

Step 2: Adopting $\boldsymbol{l}_h = \hat{e}_{\boldsymbol{u}}^{n+1}$ in (4.24) gives

$$\begin{aligned}
&\frac{1}{4\tau}(\|\hat{e}_{\boldsymbol{u}}^{n+1}\|_{L^2}^2 - \|e_{\boldsymbol{u}}^{n}\|_{L^2}^2 + \|2\hat{e}_{\boldsymbol{u}}^{n+1} - e_{\boldsymbol{u}}^{n}\|_{L^2}^2 - \|2e_{\boldsymbol{u}}^{n} - e_{\boldsymbol{u}}^{n-1}\|_{L^2}^2) + \mu \|\nabla \hat{e}_{\boldsymbol{u}}^{n+1}\|_{L^2}^2 - \big(e_p^n, \nabla \cdot \hat{e}_{\boldsymbol{u}}^{n+1}\big) \\
\leqslant& -\big[M_e^{n+1} b(\widetilde{\boldsymbol{u}}^{n+1}, \widetilde{\boldsymbol{u}}^{n+1}, \hat{e}_{\boldsymbol{u}}^{n+1}) - M^{n+1} b(\widetilde{\boldsymbol{u}}_h^{n+1}, \widetilde{\boldsymbol{u}}_h^{n+1}, \hat{e}_{\boldsymbol{u}}^{n+1})\big] + \mu\big(\nabla(\widehat{\boldsymbol{R}_h \boldsymbol{u}^{n+1}} - \boldsymbol{R}_h \boldsymbol{u}^{n+1}), \nabla \hat{e}_{\boldsymbol{u}}^{n+1}\big) \\
&- \frac{1}{\mu_0}\big[M_e^{n+1}\big(\widetilde{\boldsymbol{H}}^{n+1} \times (\nabla \times \widetilde{\boldsymbol{H}}^{n+1}), \hat{e}_{\boldsymbol{u}}^{n+1}\big) - M^{n+1}\big(\widetilde{\boldsymbol{H}}_h^{n+1} \times (\nabla \times \widetilde{\boldsymbol{H}}_h^{n+1}), \hat{e}_{\boldsymbol{u}}^{n+1}\big)\big] \\
&- \big(R_h p^n - R_h p^{n+1}, \nabla \cdot \hat{e}_{\boldsymbol{u}}^{n+1}\big) + \frac{3}{2\tau}\big(\widehat{\boldsymbol{R}_h \boldsymbol{u}^{n+1}} - \boldsymbol{R}_h \boldsymbol{u}^{n+1}, \hat{e}_{\boldsymbol{u}}^{n+1}\big) + \mathcal{T}_{\boldsymbol{u}}^{n+1}(\hat{e}_{\boldsymbol{u}}^{n+1}) \\
:=& \sum_{i=1}^{6} I_{2,i}. \qquad (4.38)
\end{aligned}$$

By the definition (2.2), we get

$$
\begin{aligned}
I_{2,1} =&\frac{1}{2}\big[M^{n+1}\big(\widetilde{\boldsymbol{u}}_h^{n+1}\cdot\nabla\widetilde{\boldsymbol{u}}_h^{n+1},\hat{e}_{\boldsymbol{u}}^{n+1}\big)-M_e^{n+1}\big(\widetilde{\boldsymbol{u}}^{n+1}\cdot\nabla\widetilde{\boldsymbol{u}}^{n+1},\hat{e}_{\boldsymbol{u}}^{n+1}\big)\big]\\
&-\frac{1}{2}\big[M^{n+1}\big(\widetilde{\boldsymbol{u}}_h^{n+1}\cdot\nabla\hat{e}_{\boldsymbol{u}}^{n+1},\widetilde{\boldsymbol{u}}_h^{n+1}\big)-M_e^{n+1}\big(\widetilde{\boldsymbol{u}}^{n+1}\cdot\nabla\hat{e}_{\boldsymbol{u}}^{n+1},\widetilde{\boldsymbol{u}}^{n+1}\big)\big]\\
=&\frac{1}{2}\big[\big(\widetilde{\boldsymbol{u}}_h^{n+1}\cdot\nabla\tilde{e}_{\boldsymbol{u}}^{n+1},\hat{e}_{\boldsymbol{u}}^{n+1}\big)+\big(\widetilde{\boldsymbol{u}}_h^{n+1}\cdot\nabla(\widetilde{\boldsymbol{u}}^{n+1}-\boldsymbol{R}_h\widetilde{\boldsymbol{u}}^{n+1}),\hat{e}_{\boldsymbol{u}}^{n+1}\big)\\
&+\big(\tilde{e}_{\boldsymbol{u}}^{n+1}\cdot\nabla\widetilde{\boldsymbol{u}}^{n+1},\hat{e}_{\boldsymbol{u}}^{n+1}\big)+\big((\widetilde{\boldsymbol{u}}^{n+1}-\boldsymbol{R}_h\widetilde{\boldsymbol{u}}^{n+1})\cdot\nabla\widetilde{\boldsymbol{u}}^{n+1},\hat{e}_{\boldsymbol{u}}^{n+1}\big)\big]\\
&-\frac{1}{2}\big[\big(\widetilde{\boldsymbol{u}}_h^{n+1}\cdot\nabla\hat{e}_{\boldsymbol{u}}^{n+1},\tilde{e}_{\boldsymbol{u}}^{n+1}\big)+\big(\widetilde{\boldsymbol{u}}_h^{n+1}\cdot\nabla\hat{e}_{\boldsymbol{u}}^{n+1},(\widetilde{\boldsymbol{u}}^{n+1}-\boldsymbol{R}_h\widetilde{\boldsymbol{u}}^{n+1})\big)\\
&+\big(\tilde{e}_{\boldsymbol{u}}^{n+1}\cdot\nabla\hat{e}_{\boldsymbol{u}}^{n+1},\widetilde{\boldsymbol{u}}^{n+1}\big)+\big((\widetilde{\boldsymbol{u}}^{n+1}-\boldsymbol{R}_h\widetilde{\boldsymbol{u}}^{n+1})\cdot\nabla\hat{e}_{\boldsymbol{u}}^{n+1},\widetilde{\boldsymbol{u}}^{n+1}\big)\\
&+\frac{1}{2}(M^{n+1}-M_e^{n+1})\big[\big(\widetilde{\boldsymbol{u}}_h^{n+1}\cdot\nabla\widetilde{\boldsymbol{u}}_h^{n+1},\hat{e}_{\boldsymbol{u}}^{n+1}\big)-\big(\widetilde{\boldsymbol{u}}_h^{n+1}\cdot\nabla\hat{e}_{\boldsymbol{u}}^{n+1},\widetilde{\boldsymbol{u}}_h^{n+1}\big)\big]\\
\leqslant&\frac{1}{2}\big[\big(\widetilde{\boldsymbol{u}}_h^{n+1}\cdot\nabla(\widetilde{\boldsymbol{u}}^{n+1}-\boldsymbol{R}_h\widetilde{\boldsymbol{u}}^{n+1}),\hat{e}_{\boldsymbol{u}}^{n+1}\big)+\|\tilde{e}_{\boldsymbol{u}}^{n+1}\|_{L^2}\|\nabla\widetilde{\boldsymbol{u}}^{n+1}\|_{L^\infty}\|\hat{e}_{\boldsymbol{u}}^{n+1}\|_{L^2}\\
&+\|\widetilde{\boldsymbol{u}}^{n+1}-\boldsymbol{R}_h\widetilde{\boldsymbol{u}}^{n+1}\|_{L^2}\|\nabla\widetilde{\boldsymbol{u}}^{n+1}\|_{L^\infty}\|\hat{e}_{\boldsymbol{u}}^{n+1}\|_{L^2}+\|\widetilde{\boldsymbol{u}}_h^{n+1}\|_{L^\infty}\|\nabla\hat{e}_{\boldsymbol{u}}^{n+1}\|_{L^2}\|\widetilde{\boldsymbol{u}}^{n+1}-\boldsymbol{R}_h\widetilde{\boldsymbol{u}}^{n+1}\|_{L^2}\\
&+\|\tilde{e}_{\boldsymbol{u}}^{n+1}\|_{L^2}\|\nabla\hat{e}_{\boldsymbol{u}}^{n+1}\|_{L^2}\|\widetilde{\boldsymbol{u}}^{n+1}\|_{L^\infty}+\|\widetilde{\boldsymbol{u}}^{n+1}-\boldsymbol{R}_h\widetilde{\boldsymbol{u}}^{n+1}\|_{L^2}\|\nabla\hat{e}_{\boldsymbol{u}}^{n+1}\|_{L^2}\|\widetilde{\boldsymbol{u}}^{n+1}\|_{L^\infty}\\
&+|M_e^{n+1}-M^{n+1}|(\|\widetilde{\boldsymbol{u}}_h^{n+1}\|_{L^\infty}\|\nabla\widetilde{\boldsymbol{u}}_h^{n+1}\|_{L^2}\|\hat{e}_{\boldsymbol{u}}^{n+1}\|_{L^2}+\|\widetilde{\boldsymbol{u}}_h^{n+1}\|_{L^2}\|\nabla\hat{e}_{\boldsymbol{u}}^{n+1}\|_{L^2}\|\widetilde{\boldsymbol{u}}_h^{n+1}\|_{L^\infty})\big]\\
\leqslant&C[h^{2r+2}+\tau^4+\|\tilde{e}_{\boldsymbol{u}}^{n+1}\|_{L^2}^2+(M_e^{n+1}-M^{n+1})^2]+\frac{\mu}{8}\|\nabla\hat{e}_{\boldsymbol{u}}^{n+1}\|_{L^2}^2\\
&+\frac{1}{2}\big(\widetilde{\boldsymbol{u}}_h^{n+1}\cdot\nabla(\widetilde{\boldsymbol{u}}^{n+1}-\boldsymbol{R}_h\widetilde{\boldsymbol{u}}^{n+1}),\hat{e}_{\boldsymbol{u}}^{n+1}\big)\\
\leqslant&C[h^{2r+2}+\tau^4+\|\tilde{e}_{\boldsymbol{u}}^{n+1}\|_{L^2}^2+(M_e^{n+1}-M^{n+1})^2]+\frac{\mu}{4}\|\nabla\hat{e}_{\boldsymbol{u}}^{n+1}\|_{L^2}^2. \qquad (4.39)
\end{aligned}
$$

In the last inequality, we have used (4.1), (4.10), (4.32), the Cauchy inequality, Hölder inequality, Poincaré inequality and the following facts

$$
\begin{aligned}
&\big(\widetilde{\boldsymbol{u}}_h^{n+1}\cdot\nabla(\widetilde{\boldsymbol{u}}^{n+1}-\boldsymbol{R}_h\widetilde{\boldsymbol{u}}^{n+1}),\hat{e}_{\boldsymbol{u}}^{n+1}\big)\\
=&\big((\nabla\cdot\widetilde{\boldsymbol{u}}_h^{n+1})(\widetilde{\boldsymbol{u}}^{n+1}-\boldsymbol{R}_h\widetilde{\boldsymbol{u}}^{n+1}),\hat{e}_{\boldsymbol{u}}^{n+1}\big)+\big(\widetilde{\boldsymbol{u}}_h^{n+1}\cdot\nabla\hat{e}_{\boldsymbol{u}}^{n+1},\widetilde{\boldsymbol{u}}^{n+1}-\boldsymbol{R}_h\widetilde{\boldsymbol{u}}^{n+1}\big)\\
\leqslant&\|\nabla\cdot\widetilde{\boldsymbol{u}}_h^{n+1}\|_{L^3}\|\widetilde{\boldsymbol{u}}^{n+1}-\boldsymbol{R}_h\widetilde{\boldsymbol{u}}^{n+1}\|_{L^2}\|\hat{e}_{\boldsymbol{u}}^{n+1}\|_{L^6}+\|\widetilde{\boldsymbol{u}}_h^{n+1}\|_{L^\infty}\|\nabla\hat{e}_{\boldsymbol{u}}^{n+1}\|_{L^2}\|\widetilde{\boldsymbol{u}}^{n+1}-\boldsymbol{R}_h\widetilde{\boldsymbol{u}}^{n+1}\|_{L^2}\\
\leqslant&Ch^{2r+2}+\frac{\mu}{8}\|\nabla\hat{e}_{\boldsymbol{u}}^{n+1}\|_{L^2}^2 \quad \text{(by (4.9))},
\end{aligned}
$$

where by (4.30) we have $\|\nabla\cdot\widetilde{\boldsymbol{u}}_h^{n+1}\|_{L^3}\leqslant C\|\widetilde{\boldsymbol{u}}_h^{n+1}\|_{W^{1,4}}\leqslant C$, and using the interpolation inequality that for any $v\in W^{1,p}$,

$$
\|v\|_{L^q}\leqslant C\|v\|_{L^p}^{1-\alpha}\|v\|_{W^{1,p}}^{\alpha}, \quad 1<p\leqslant q<\infty, \quad \alpha=\frac{d}{p}-\frac{d}{q}\leqslant 1, \qquad (4.40)
$$

i.e., $\|\hat{e}_{\boldsymbol{u}}^{n+1}\|_{L^6}\leqslant C\|\hat{e}_{\boldsymbol{u}}^{n+1}\|_{H^1}\leqslant C\|\nabla\hat{e}_{\boldsymbol{u}}^{n+1}\|_{L^2}$ is valid.

By (4.16) we have

$$
\begin{aligned}
I_{2,2}=&\frac{2\mu\tau}{3}\big(\nabla(\nabla_hR_hp^{n+1}-\nabla_hR_hp^n),\nabla\hat{e}_{\boldsymbol{u}}^{n+1}\big)\\
\leqslant&C\tau^2\|\nabla(\nabla_hR_hp^{n+1}-\nabla_hR_hp^n)\|_{L^2}^2+\frac{\mu}{4}\|\nabla\hat{e}_{\boldsymbol{u}}^{n+1}\|_{L^2}^2\\
\leqslant&C\tau^4+\frac{\mu}{4}\|\nabla\hat{e}_{\boldsymbol{u}}^{n+1}\|_{L^2}^2, \qquad (4.41)
\end{aligned}
$$

where the term $\|\nabla(\nabla_h R_h p^{n+1} - \nabla_h R_h p^n)\|_{L^2}$ is controlled by

$$
\begin{aligned}
&\|\nabla(\nabla_h R_h p^{n+1} - \nabla_h R_h p^n)\|_{L^2}\\
\leqslant& C\tau \|\nabla(\nabla_h R_h \partial_t p)\|_{L^2} \quad \text{(by Taylor expansion and } p \text{ for } p^{n+1} \text{ in short)}\\
\leqslant& C\tau\big(\|\nabla(\nabla_h R_h \partial_t p - \nabla_h P_h \partial_t p)\|_{L^2} + \|\nabla(\nabla_h P_h \partial_t p - P_h \nabla \partial_t p)\|_{L^2} + \|\nabla P_h \nabla \partial_t p)\|_{L^2}\big)\\
\leqslant& C\tau\big(Ch^{-2}\|R_h\partial_t p - P_h \partial_t p\|_{L^2} + Ch^{-1}\|\nabla_h P_h \partial_t p - P_h\nabla\partial_t p\|_{L^2} + \|P_h \nabla \partial_t p\|_{H^1}\big) \quad \text{(by (4.14) and (4.15))}\\
\leqslant& C\tau\big(Ch^{-2}\|R_h\partial_t p - \partial_t p\|_{L^2} + Ch^{-2}\|P_h\partial_t p - \partial_t p\|_{L^2} + Ch^{-1}Ch^1 + C\|\nabla\partial_t p\|_{H^1}\big) \quad \text{(by (4.7) and (4.27))}\\
\leqslant& C\tau\big(Ch^{-2}h^2 + Ch^{-2}h^2 + C + C\big) \quad \text{(by (4.8) and (4.12))}\\
\leqslant& C\tau.
\end{aligned}
\tag{4.42}
$$

The regularity assumption (4.1) has been used frequently in the derivation.

Another nonlinear term could be analyzed as

$$
\begin{aligned}
I_{2,3} =& \big((\widetilde{\boldsymbol{H}}^{n+1} - \Pi_h \widetilde{\boldsymbol{H}}^{n+1}) \times (\nabla \times \widetilde{\boldsymbol{H}}^{n+1}), \hat{e}_{\boldsymbol{u}}^{n+1}\big) + \big(\tilde{e}_{\boldsymbol{H}}^{n+1} \times (\nabla \times \widetilde{\boldsymbol{H}}^{n+1}), \hat{e}_{\boldsymbol{u}}^{n+1}\big)\\
&+ \big(\widetilde{\boldsymbol{H}}_h^{n+1} \times (\nabla \times (\widetilde{\boldsymbol{H}}^{n+1} - \Pi_h \widetilde{\boldsymbol{H}}^{n+1})), \hat{e}_{\boldsymbol{u}}^{n+1}\big) + \big(\widetilde{\boldsymbol{H}}_h^{n+1} \times (\nabla \times \tilde{e}_{\boldsymbol{H}}^{n+1}), \hat{e}_{\boldsymbol{u}}^{n+1}\big)\\
&+ (M_e^{n+1} - M^{n+1})\big(\widetilde{\boldsymbol{H}}_h^{n+1} \times (\nabla \times \widetilde{\boldsymbol{H}}_h^{n+1}), \hat{e}_{\boldsymbol{u}}^{n+1}\big)\\
\leqslant& \|\widetilde{\boldsymbol{H}}^{n+1} - \Pi_h \widetilde{\boldsymbol{H}}^{n+1}\|_{L^2} \|\nabla \times \widetilde{\boldsymbol{H}}^{n+1}\|_{L^\infty} \|\hat{e}_{\boldsymbol{u}}^{n+1}\|_{L^2} + \|\tilde{e}_{\boldsymbol{H}}^{n+1}\|_{L^2} \|\nabla \times \widetilde{\boldsymbol{H}}^{n+1}\|_{L^\infty} \|\hat{e}_{\boldsymbol{u}}^{n+1}\|_{L^2}\\
&+ \big(\widetilde{\boldsymbol{H}}_h^{n+1} \times (\nabla \times (\widetilde{\boldsymbol{H}}^{n+1} - \Pi_h \widetilde{\boldsymbol{H}}^{n+1})), \hat{e}_{\boldsymbol{u}}^{n+1}\big) + \big(\widetilde{\boldsymbol{H}}_h^{n+1} \times (\nabla \times \tilde{e}_{\boldsymbol{H}}^{n+1}), \hat{e}_{\boldsymbol{u}}^{n+1}\big)\\
&+ |M_e^{n+1} - M^{n+1}| \|\widetilde{\boldsymbol{H}}_h^{n+1}\|_{L^2} \|\nabla \times \widetilde{\boldsymbol{H}}_h^{n+1}\|_{L^3} \|\hat{e}_{\boldsymbol{u}}^{n+1}\|_{L^6}\\
\leqslant& C(h^{r+1} + \|\tilde{e}_{\boldsymbol{H}}^{n+1}\|_{L^2} + |M_e^{n+1} - M^{n+1}|)\|\nabla \hat{e}_{\boldsymbol{u}}^{n+1}\|_{L^2} \quad \text{(by (4.13) and Poincaré inequality)}\\
&+ |\big(\widetilde{\boldsymbol{H}}_h^{n+1} \times (\nabla \times \hat{e}_{\boldsymbol{u}}^{n+1}), \widetilde{\boldsymbol{H}}^{n+1} - \Pi_h \widetilde{\boldsymbol{H}}^{n+1}\big)| + |\big(\hat{e}_{\boldsymbol{u}}^{n+1} \times (\nabla \times \widetilde{\boldsymbol{H}}_h^{n+1}), \widetilde{\boldsymbol{H}}^{n+1} - \Pi_h \widetilde{\boldsymbol{H}}^{n+1}\big)|\\
&+ |\big(\widetilde{\boldsymbol{H}}_h^{n+1} \times \tilde{e}_{\boldsymbol{H}}^{n+1}, \nabla \times \hat{e}_{\boldsymbol{u}}^{n+1}\big)| + |\big(\hat{e}_{\boldsymbol{u}}^{n+1} \times \tilde{e}_{\boldsymbol{H}}^{n+1}, \nabla \times \widetilde{\boldsymbol{H}}_h^{n+1}\big)| \quad \text{(by integration inparts)}\\
\leqslant& C(h^{2r+2} + \|\tilde{e}_{\boldsymbol{H}}^{n+1}\|_{L^2}^2 + (M_e^{n+1} - M^{n+1})^2) + \frac{\mu}{8}\|\nabla \hat{e}_{\boldsymbol{u}}^{n+1}\|_{L^2}^2\\
&+ \|\widetilde{\boldsymbol{H}}_h^{n+1}\|_{L^\infty} \|\nabla \times \hat{e}_{\boldsymbol{u}}^{n+1}\|_{L^2} \|\widetilde{\boldsymbol{H}}^{n+1} - \Pi_h \widetilde{\boldsymbol{H}}^{n+1}\|_{L^2}\\
&+ \|\hat{e}_{\boldsymbol{u}}^{n+1}\|_{L^6} \|\nabla \times \widetilde{\boldsymbol{H}}_h^{n+1}\|_{L^3} \|\widetilde{\boldsymbol{H}}^{n+1} - \Pi_h \widetilde{\boldsymbol{H}}^{n+1}\|_{L^2}\\
&+ \|\widetilde{\boldsymbol{H}}_h^{n+1}\|_{L^\infty} \|\tilde{e}_{\boldsymbol{H}}^{n+1}\|_{L^2} \|\nabla \times \hat{e}_{\boldsymbol{u}}^{n+1}\|_{L^2} + \|\hat{e}_{\boldsymbol{u}}^{n+1}\|_{L^6} \|\tilde{e}_{\boldsymbol{H}}^{n+1}\|_{L^2} \|\nabla \times \widetilde{\boldsymbol{H}}_h^{n+1}\|_{L^3}\\
\leqslant& C[h^{2r+2} + \|\tilde{e}_{\boldsymbol{H}}^{n+1}\|_{L^2}^2 + (M_e^{n+1} - M^{n+1})^2] + \frac{\mu}{4}\|\nabla \hat{e}_{\boldsymbol{u}}^{n+1}\|_{L^2}^2,
\end{aligned}
\tag{4.43}
$$

where in the last inequality we have utilized (4.31), (4.40) and the Poincaré inequality.

Similarly, by (4.16) we obtain

$$
I_{2,4} + I_{2,5} = -\frac{3}{2}\Big(\frac{\boldsymbol{R}_h \boldsymbol{u}^{n+1} - \widehat{\boldsymbol{R}_h \boldsymbol{u}^{n+1}}}{\tau}, \hat{e}_{\boldsymbol{u}}^{n+1}\Big) - \big(\nabla_h R_h p^{n+1} - \nabla_h R_h p^n, \hat{e}_{\boldsymbol{u}}^{n+1}\big) = 0. \tag{4.44}
$$

Finally, the term associated with the truncation error $\mathcal{T}_{\boldsymbol{u}}^{n+1}$ could be bounded by

$$
\mathcal{T}_{\boldsymbol{u}}^{n+1} \leqslant C(h^{2r+2} + \tau^4 + \|e_{\boldsymbol{u}}^{n+1}\|_{L^2}^2) + \frac{\mu}{8}\|\nabla \hat{e}_{\boldsymbol{u}}^{n+1}\|_{L^2}^2. \tag{4.45}
$$

Thus, (4.38) is simplified by (4.39),(4.41),(4.43)-(4.45) as

$$
\begin{aligned}
&\frac{1}{4\tau}(\|\hat{e}_{\boldsymbol{u}}^{n+1}\|_{L^2}^2 - \|e_{\boldsymbol{u}}^{n}\|_{L^2}^2 + \|2\hat{e}_{\boldsymbol{u}}^{n+1} - e_{\boldsymbol{u}}^{n}\|_{L^2}^2 - \|2e_{\boldsymbol{u}}^{n} - e_{\boldsymbol{u}}^{n-1}\|_{L^2}^2)\\
&+ \frac{\mu}{8}\|\nabla \hat{e}_{\boldsymbol{u}}^{n+1}\|_{L^2}^2 - \big(e_p^n, \nabla \cdot \hat{e}_{\boldsymbol{u}}^{n+1}\big)\\
\leqslant& C[h^{2r+2} + \tau^4 + \|\tilde{e}_{\boldsymbol{u}}^{n+1}\|_{L^2}^2 + \|\tilde{e}_{\boldsymbol{H}}^{n+1}\|_{L^2}^2 + (M_e^{n+1} - M^{n+1})^2 + \|e_{\boldsymbol{u}}^{n+1}\|_{L^2}^2].
\end{aligned}
\tag{4.46}
$$

Step 3: A combination of (4.16), (4.26) and (4.25) indicates that

$$\nabla \cdot \hat{e}_{\boldsymbol{u}}^{n+1} = \frac{2\tau}{3}\nabla \cdot \nabla_h (e_p^{n+1} - e_p^n),$$

which leads to

$$-(e_p^n, \nabla \cdot \hat{e}_{\boldsymbol{u}}^{n+1}) = \frac{\tau}{3}(\|\nabla_h e_p^{n+1}\|_{L^2}^2 - \|\nabla_h e_p^n\|_{L^2}^2 - \|\nabla_h (e_p^{n+1} - e_p^n)\|_{L^2}^2). \tag{4.47}$$

Again by (4.26), (4.25) yields

$$\|\hat{e}_{\boldsymbol{u}}^{n+1}\|_{L^2}^2 = \|e_{\boldsymbol{u}}^{n+1}\|_{L^2}^2 + \frac{4\tau^2}{9}\|\nabla_h (e_p^{n+1} - e_p^n)\|_{L^2}^2 \quad \text{and} \tag{4.48}$$

$$\|2\hat{e}_{\boldsymbol{u}}^{n+1} - e_{\boldsymbol{u}}^n\|_{L^2}^2 = \|2e_{\boldsymbol{u}}^{n+1} - e_{\boldsymbol{u}}^n\|_{L^2} + \frac{16\tau^2}{9}\|\nabla_h (e_p^{n+1} - e_p^n)\|_{L^2}^2. \tag{4.49}$$

Step 4: Now we need to estimate $M_e^{n+1} - M^{n+1} := e_M^{n+1}$. Subtracting (4.21) from (3.6) yields

$$\begin{aligned}
\frac{3e_M^{n+1} - 4e_M^n + e_M^{n-1}}{2\tau} =& \mu_0[b(\widetilde{\boldsymbol{u}}^{n+1}, \widetilde{\boldsymbol{u}}^{n+1}, \boldsymbol{u}^{n+1}) - b(\widetilde{\boldsymbol{u}}_h^{n+1}, \widetilde{\boldsymbol{u}}_h^{n+1}, \hat{\boldsymbol{u}}_h^{n+1})] + T_M \\
&+ [(\widetilde{\boldsymbol{H}}^{n+1} \times (\nabla \times \widetilde{\boldsymbol{H}}^{n+1}), \boldsymbol{u}^{n+1}) - (\widetilde{\boldsymbol{H}}_h^{n+1} \times (\nabla \times \widetilde{\boldsymbol{H}}_h^{n+1}), \hat{\boldsymbol{u}}_h^{n+1})] \\
&- [(\widetilde{\boldsymbol{u}}^{n+1} \times \widetilde{\boldsymbol{H}}^{n+1}, \nabla \times \boldsymbol{H}^{n+1}) - (\widetilde{\boldsymbol{u}}_h^{n+1} \times \widetilde{\boldsymbol{H}}_h^{n+1}, \nabla \times \boldsymbol{H}_h^{n+1})] \\
:=& \sum_{i=1}^{4} I_{4,i}.
\end{aligned} \tag{4.50}$$

The definition (2.2) implies that

$$\begin{aligned}
I_{4,1} =& \frac{\mu_0}{2}\big[(\widetilde{\boldsymbol{u}}^{n+1} \cdot \nabla \widetilde{\boldsymbol{u}}^{n+1}, \boldsymbol{u}^{n+1}) - (\widetilde{\boldsymbol{u}}_h^{n+1} \cdot \nabla \widetilde{\boldsymbol{u}}_h^{n+1}, \hat{\boldsymbol{u}}_h^{n+1})\big] \\
&- \frac{\mu_0}{2}\big[(\widetilde{\boldsymbol{u}}^{n+1} \cdot \nabla \boldsymbol{u}^{n+1}, \widetilde{\boldsymbol{u}}^{n+1}) - (\widetilde{\boldsymbol{u}}_h^{n+1} \cdot \nabla \hat{\boldsymbol{u}}_h^{n+1}, \widetilde{\boldsymbol{u}}_h^{n+1})\big] \\
=& \frac{\mu_0}{2}\big[((\widetilde{\boldsymbol{u}}^{n+1} - \widetilde{\boldsymbol{R}}_h \boldsymbol{u}^{n+1}) \cdot \nabla \widetilde{\boldsymbol{u}}^{n+1}, \boldsymbol{u}^{n+1}) + (\widetilde{e}_{\boldsymbol{u}}^{n+1} \cdot \nabla \widetilde{\boldsymbol{u}}^{n+1}, \boldsymbol{u}^{n+1}) \\
&+ (\widetilde{\boldsymbol{u}}_h^{n+1} \cdot \nabla (\widetilde{\boldsymbol{u}}^{n+1} - \boldsymbol{R}_h \widetilde{\boldsymbol{u}}^{n+1}), \boldsymbol{u}^{n+1}) + (\widetilde{\boldsymbol{u}}_h^{n+1} \cdot \nabla \widetilde{e}_{\boldsymbol{u}}^{n+1}, \boldsymbol{u}^{n+1}) \\
&+ (\widetilde{\boldsymbol{u}}_h^{n+1} \cdot \nabla \widetilde{\boldsymbol{u}}_h^{n+1}, \boldsymbol{u}^{n+1} - \boldsymbol{R}_h \boldsymbol{u}^{n+1}) + (\widetilde{\boldsymbol{u}}_h^{n+1} \cdot \nabla \widetilde{\boldsymbol{u}}_h^{n+1}, e_{\boldsymbol{u}}^{n+1}) \\
&+ (\widetilde{\boldsymbol{u}}_h^{n+1} \cdot \nabla \widetilde{\boldsymbol{u}}_h^{n+1}, \boldsymbol{u}_h^{n+1} - \hat{\boldsymbol{u}}_h^{n+1})\big] - \frac{\mu_0}{2}\big[((\widetilde{\boldsymbol{u}}^{n+1} - \boldsymbol{R}_h \widetilde{\boldsymbol{u}}^{n+1}) \cdot \nabla \boldsymbol{u}^{n+1}, \widetilde{\boldsymbol{u}}^{n+1}) \\
&+ (\widetilde{e}_{\boldsymbol{u}}^{n+1} \cdot \nabla \boldsymbol{u}^{n+1}, \widetilde{\boldsymbol{u}}^{n+1}) + (\widetilde{\boldsymbol{u}}_h^{n+1} \cdot \nabla \boldsymbol{u}^{n+1}, \widetilde{\boldsymbol{u}}^{n+1} - \boldsymbol{R}_h \widetilde{\boldsymbol{u}}^{n+1}) \\
&+ (\widetilde{\boldsymbol{u}}_h^{n+1} \cdot \nabla \boldsymbol{u}^{n+1}, \widetilde{e}_{\boldsymbol{u}}^{n+1}) + (\widetilde{\boldsymbol{u}}_h^{n+1} \cdot \nabla (\boldsymbol{u}^{n+1} - \boldsymbol{R}_h \boldsymbol{u}^{n+1}), \widetilde{\boldsymbol{u}}_h^{n+1}) \\
&+ (\widetilde{\boldsymbol{u}}_h^{n+1} \cdot \nabla e_{\boldsymbol{u}}^{n+1}, \widetilde{\boldsymbol{u}}_h^{n+1}) + (\widetilde{\boldsymbol{u}}_h^{n+1} \cdot \nabla (\boldsymbol{u}_h^{n+1} - \hat{\boldsymbol{u}}_h^{n+1}), \widetilde{\boldsymbol{u}}_h^{n+1})\big] \\
\leqslant& C(h^{r+1} + \tau^2 + \|\widetilde{e}_{\boldsymbol{u}}^{n+1}\|_{L^2} + \|e_{\boldsymbol{u}}^{n+1}\|_{L^2} + \|\hat{e}_{\boldsymbol{u}}^{n+1}\|_{L^2}),
\end{aligned} \tag{4.51}$$

where we have used the Hölder inequality, integration by parts and the following estimate

$$\begin{aligned}
\|\boldsymbol{u}_h^{n+1} - \hat{\boldsymbol{u}}_h^{n+1}\|_{L^2} \leqslant& \|\boldsymbol{u}_h^{n+1} - \boldsymbol{R}_h \boldsymbol{u}^{n+1}\|_{L^2} + \|\boldsymbol{R}_h \boldsymbol{u}^{n+1} - \widehat{\boldsymbol{u}_h^{n+1}}\|_{L^2} + \|\widehat{\boldsymbol{u}_h^{n+1}} - \hat{\boldsymbol{u}}_h^{n+1}\|_{L^2} \\
\leqslant& \|e_{\boldsymbol{u}}^{n+1}\|_{L^2} + \|\hat{e}_{\boldsymbol{u}}^{n+1}\|_{L^2} + \frac{2\tau}{3}\|\nabla_h (R_h p^{n+1} - R_h p^n)\|_{L^2} \quad \text{(by (4.16))} \\
\leqslant& \|e_{\boldsymbol{u}}^{n+1}\|_{L^2} + \|\hat{e}_{\boldsymbol{u}}^{n+1}\|_{L^2} + C\tau^2 \quad \text{(by (4.28))}.
\end{aligned} \tag{4.52}$$

The truncation term could be controlled directly by

$$I_{4,2} \leqslant C\tau^2. \tag{4.53}$$

Next for $I_{4,3}$ we have

$$\begin{aligned}
I_{4,3} =&\big((\widetilde{\boldsymbol{H}}^{n+1} - \Pi_h\widetilde{\boldsymbol{H}}^{n+1}) \times (\nabla \times \widetilde{\boldsymbol{H}}^{n+1}), \boldsymbol{u}^{n+1}\big) + \big(\tilde{e}_{\boldsymbol{H}}^{n+1} \times (\nabla \times \widetilde{\boldsymbol{H}}^{n+1}), \boldsymbol{u}^{n+1}\big)\\
&+ \big(\widetilde{\boldsymbol{H}}_h^{n+1} \times (\nabla \times (\widetilde{\boldsymbol{H}}^{n+1} - \Pi_h\widetilde{\boldsymbol{H}}^{n+1})), \boldsymbol{u}^{n+1}\big) + \big(\widetilde{\boldsymbol{H}}_h^{n+1} \times (\nabla \times \tilde{e}_{\boldsymbol{H}}^{n+1}), \boldsymbol{u}^{n+1}\big)\\
&+ \big(\widetilde{\boldsymbol{H}}_h^{n+1} \times (\nabla \times \widetilde{\boldsymbol{H}}_h^{n+1}), \boldsymbol{u}^{n+1} - \boldsymbol{R}_h\boldsymbol{u}^{n+1}\big) + \big(\widetilde{\boldsymbol{H}}_h^{n+1} \times (\nabla \times \widetilde{\boldsymbol{H}}_h^{n+1}), e_{\boldsymbol{u}}^{n+1}\big)\\
&+ \big(\widetilde{\boldsymbol{H}}_h^{n+1} \times (\nabla \times \widetilde{\boldsymbol{H}}_h^{n+1})\boldsymbol{u}_h^{n+1} - \hat{\boldsymbol{u}}_h^{n+1}\big)\\
\leqslant& C(h^{r+1} + \tau^2 + \|\tilde{e}_{\boldsymbol{H}}^{n+1}\|_{L^2} + \|e_{\boldsymbol{u}}^{n+1}\|_{L^2}),
\end{aligned} \tag{4.54}$$

where (4.52) has been utilized.

Similarly, the following inequality could be derived

$$I_{4,4} \leqslant C(h^{r+1} + \|e_{\boldsymbol{H}}^{n+1}\|_{L^2} + \|e_{\boldsymbol{u}}^{n+1}\|_{L^2}), \tag{4.55}$$

and we skip the proof for simplicity.

From (4.51), (4.53), (4.54) and (4.55), taking the inner product with e_M^{n+1} by (4.50) leads to

$$\begin{aligned}
&\frac{1}{4\tau}[(e_M^{n+1})^2 - (e_M^n)^2 + (2e_M^{n+1} - e_M^n)^2 - (2e_M^n - e_M^{n-1})^2]\\
\leqslant& C(h^{2r+2} + \tau^4 + \|\tilde{e}_{\boldsymbol{u}}^{n+1}\|_{L^2}^2 + \|\tilde{e}_{\boldsymbol{H}}^{n+1}\|_{L^2}^2 + \|e_{\boldsymbol{u}}^{n+1}\|_{L^2}^2 + \|e_{\boldsymbol{H}}^{n+1}\|_{L^2}^2 + (e_M^{n+1})^2) + \frac{\mu}{8}\|\nabla\hat{e}_{\boldsymbol{u}}^{n+1}\|_{L^2}^2,
\end{aligned} \tag{4.56}$$

where the Cauchy inequality and Poincaré inequality have been adopted.

Step 5: A combination of (4.37), (4.46)-(4.49) and (4.56) leads to

$$\begin{aligned}
&\frac{1}{4\tau}[\|e_{\boldsymbol{H}}^{n+1}\|_{L^2}^2 - \|e_{\boldsymbol{H}}^n\|_{L^2}^2 + \|2e_{\boldsymbol{H}}^{n+1} - e_{\boldsymbol{H}}^n\|_{L^2}^2 - \|2e_{\boldsymbol{H}}^n - e_{\boldsymbol{H}}^{n-1}\|_{L^2}^2 + \|e_{\boldsymbol{u}}^{n+1}\|_{L^2}^2 - \|e_{\boldsymbol{u}}^n\|_{L^2}^2\\
&+ \|2e_{\boldsymbol{u}}^{n+1} - e_{\boldsymbol{u}}^n\|_{L^2}^2 - \|2e_{\boldsymbol{u}}^n - e_{\boldsymbol{u}}^{n-1}\|_{L^2}^2 + (e_M^{n+1})^2 - (e_M^n)^2 + (2e_M^{n+1} - e_M^n)^2 - (2e_M^n - e_M^{n-1})^2]\\
&+ \frac{2\tau}{9}(\|\nabla_h e_p^{n+1}\|_{L^2}^2 - \|\nabla_h e_p^n\|_{L^2}^2) + \frac{\eta}{2\mu_0}\|\nabla \times e_{\boldsymbol{H}}^{n+1}\|_{L^2}^2 + \frac{\eta}{\mu_0}\|\nabla \cdot e_{\boldsymbol{H}}^{n+1}\|_{L^2}^2 + \frac{\eta_2}{2\mu_0}\|e_{\boldsymbol{\phi}}^{n+1}\|_{L^2}^2\\
\leqslant& C[(h^{r+1} + \tau^2)^2 + \|\tilde{e}_{\boldsymbol{u}}^{n+1}\|_{L^2}^2 + \|\tilde{e}_{\boldsymbol{H}}^{n+1}\|_{L^2}^2 + \|e_{\boldsymbol{u}}^{n+1}\|_{L^2}^2 + \|e_{\boldsymbol{H}}^{n+1}\|_{L^2}^2 + (e_M^{n+1})^2],
\end{aligned} \tag{4.57}$$

for $n = 1, 2, ...N$.

An application of the discrete Gronwall's inequality results in

$$\|e_{\boldsymbol{H}}^{n+1}\|_{L^2}^2 + \|e_{\boldsymbol{u}}^{n+1}\|_{L^2}^2 \leqslant C(h^{r+1} + \tau^2)^2, \tag{4.58}$$

for $\tau < \tau_0$ and $h < h_0$, where τ_0 and h_0 are positive constants. This has recovered the induction assumption (4.29) when $m = n + 1$.

Together with the projection estimates (4.7)-(4.13), we finish the proof of Theorem 4.1.

□

5 Numerical examples

The computations are carried out by using the software *FreeFEM++*.

5.1 Accuracy test

For the sake of brevity, we consider the incompressible resistive MHD equations

$$\partial_t \boldsymbol{H} + \frac{\eta}{\mu_0}\nabla\times(\nabla\times\boldsymbol{H}) + \frac{\eta_2}{\mu_0}\nabla\times(\nabla\times(\nabla\times(\nabla\times\boldsymbol{H}))) - \nabla\times(\boldsymbol{u}\times\boldsymbol{H}) = \boldsymbol{J}, \tag{5.1}$$

$$\partial_t \boldsymbol{u} + \boldsymbol{u}\cdot\nabla\boldsymbol{u} - \mu\Delta\boldsymbol{u} + \nabla p + \frac{1}{\mu_0}\boldsymbol{H}\times(\nabla\times\boldsymbol{H}) = \boldsymbol{f}, \tag{5.2}$$

$$\nabla\cdot\boldsymbol{H} = 0, \quad \nabla\cdot\boldsymbol{u} = 0, \tag{5.3}$$

in a two-dimensional domain $[0,2\pi]\times[0,2\pi]$, with the initial and boundary conditions (1.4)-(1.5). Here $\boldsymbol{J}$ and $\boldsymbol{f}$ are the source terms, and are determined by the given exact solution

$$\begin{aligned} \boldsymbol{u} &= t^8\begin{pmatrix} \sin^2 x\sin(2y) \\ -\sin(2x)\sin^2 y\end{pmatrix}, \\ \boldsymbol{H} &= t^5\begin{pmatrix} -\sin y\cos x \\ \sin x\cos y\end{pmatrix}, \\ p &= t^5\sin(2x)\sin(2y). \end{aligned} \tag{5.4}$$

Note that the above exact solutions $\boldsymbol{u}$ and $\boldsymbol{H}$ satisfy the divergence-free conditions.

Example 1: All the coefficients in (5.1)-(5.3) are chosen to be 1, and we take the final time $T = 1$. We first solve the MHD system (5.1)-(5.3) by the scheme (3.1)-(3.4) with a quadratic finite element approximation for $\boldsymbol{H}$ and $\boldsymbol{u}$, and a linear finite element approximation for p. To impose the boundary condition $\boldsymbol{H}\times\boldsymbol{n} = 0$, we make use of the definition directly. For example, on the edge $\{(x,y) : 0 \leqslant x \leqslant 2\pi, y = 0\}$, $\boldsymbol{n} = (0,-1)^T$ and denoted by $\boldsymbol{H} := (H_1, H_2)^T$, then we have $H_1 = 0$. To emphasize the convergence rate in time, a sufficiently small spatial mesh size $h = 2\pi/100$ is chosen such that the spatial discretization error can be relatively negligible. The time step is $\tau = T/N$ with $N = 40, 80, 160, 320$. We present the numerical results at time $T = 1$ in Table 1(a), which indicate that the proposed scheme is convergent at a second-order temporally accuracy.

(a) Temporal convergence rates

τ	$\|\boldsymbol{H}^N - \boldsymbol{H}_h^N\|_{L^2}$	Order	$\|\boldsymbol{u}^N - \boldsymbol{u}_h^N\|_{L^2}$	Order
1/40	6.969×10^{-3}		2.418×10^{-2}	
1/80	1.797×10^{-3}	1.96	6.383×10^{-3}	1.92
1/160	4.561×10^{-4}	1.98	1.641×10^{-3}	1.96
1/320	1.158×10^{-4}	1.98	4.211×10^{-4}	1.96

(b) Spatial convergence rates

h	$\|\boldsymbol{H}^N - \boldsymbol{H}_h^N\|_{L^2}$	Order	$\|\boldsymbol{u}^N - \boldsymbol{u}_h^N\|_{L^2}$	Order
$2\pi/10$	1.678×10^{-2}		9.111×10^{-2}	
$2\pi/20$	2.153×10^{-3}	2.96	9.570×10^{-3}	3.25
$2\pi/40$	2.703×10^{-4}	2.99	1.195×10^{-3}	3.00
$2\pi/80$	3.388×10^{-5}	3.00	1.502×10^{-4}	2.99

Table 1: $\eta = \eta_2 = \mu = \mu_0 = 1$.

Then we solve the problem (5.1)-(5.3) by the scheme (3.1)-(3.4) with a sufficiently small temporal step $\tau = 1/2000$, to observe the spatial convergence rate. Take spatial size as $h = 1/10, 1/20, 1/40, 1/80$. Again, a quadratic finite element approximation for $\boldsymbol{H}$ and $\boldsymbol{u}$ is adopted, combined with a linear finite element approximation for p. Numerical results at $T = 1$ are displayed in Table 1(b). It is clearly seen that the spatial numerical errors are approximately $O(h^3)$, which is consistent with the theoretical analysis in Theorem 4.1.

Next some experiments with small parameters are provided to verify the robustness of the proposed scheme. We still consider the space domain $[0, 2\pi] \times [0, 2\pi] \times [0, 1]$ and use the exact solution (5.4) to test the accuracy.

Example 2: Adopt the same parameters in Example 1 except the viscosity $\mu = 0.01$ instead of $\mu = 1$, and then the numerical results are shown in Tables 2(a) and 2(b).

(a) Temporal convergence rates, $h = 2\pi/100$

τ	$\\|\boldsymbol{H}^N - \boldsymbol{H}_h^N\\|_{L^2}$	Order	$\\|\boldsymbol{u}^N - \boldsymbol{u}_h^N\\|_{L^2}$	Order
1/40	6.825×10^{-3}		4.007×10^{-2}	
1/80	1.757×10^{-3}	1.96	1.056×10^{-3}	1.92
1/160	4.457×10^{-4}	1.98	2.756×10^{-3}	1.94

(b) Spatial convergence rates, $\tau = 1/2000$

h	$\\|\boldsymbol{H}^N - \boldsymbol{H}_h^N\\|_{L^2}$	Order	$\\|\boldsymbol{u}^N - \boldsymbol{u}_h^N\\|_{L^2}$	Order
$2\pi/10$	1.601×10^{-2}		6.358×10^{-1}	
$2\pi/20$	2.121×10^{-3}	2.92	1.412×10^{-1}	2.17
$2\pi/40$	2.691×10^{-4}	2.98	1.545×10^{-2}	3.19

Table 2: $\mu = 0.01, \eta = \eta_2 = \mu_0 = 1$

Example 3: Further, except for a small hyper-resistivity $\eta_2 = 0.01$, we still take the same parameters in Example 1, and then obtain the results in Tables 3(a) and 3(b).

(a) Temporal convergence rates, $h = 2\pi/100$

τ	$\\|\boldsymbol{H}^N - \boldsymbol{H}_h^N\\|_{L^2}$	Order	$\\|\boldsymbol{u}^N - \boldsymbol{u}_h^N\\|_{L^2}$	Order
1/40	1.448×10^{-2}		2.379×10^{-2}	
1/80	3.791×10^{-3}	1.93	6.285×10^{-3}	1.92
1/160	9.703×10^{-4}	1.97	1.615×10^{-3}	1.96

(b) Spatial convergence rates, $\tau = 1/2000$

h	$\\|\boldsymbol{H}^N - \boldsymbol{H}_h^N\\|_{L^2}$	Order	$\\|\boldsymbol{u}^N - \boldsymbol{u}_h^N\\|_{L^2}$	Order
$2\pi/10$	1.585×10^{-2}		9.122×10^{-2}	
$2\pi/20$	2.109×10^{-3}	2.91	9.571×10^{-3}	3.25
$2\pi/40$	2.691×10^{-4}	2.97	1.195×10^{-3}	3.00

Table 3: $\eta_2 = 0.01, \eta = \mu = \mu_0 = 1$

Example 4: Now we adopt $\eta = 0.1$ and $\eta_2 = 0.001$ and keep other parameters in Example 1 unchanged. Then the numerical results are shown in Tables 4(a) and 4(b) as follows.

All the numerical results are consistent with the theoretical results proven in Theorem 4.1.

(a) Temporal convergence rates, $h = 2\pi/100$

τ	$\|\boldsymbol{H}^N - \boldsymbol{H}_h^N\|_{L^2}$	Order	$\|\boldsymbol{u}^N - \boldsymbol{u}_h^N\|_{L^2}$	Order
$1/40$	2.274×10^{-2}		2.343×10^{-2}	
$1/80$	5.976×10^{-3}	1.93	6.186×10^{-3}	1.92
$1/160$	1.534×10^{-3}	1.96	1.589×10^{-3}	1.96

(b) Spatial convergence rates, $\tau = 1/2000$

h	$\|\boldsymbol{H}^N - \boldsymbol{H}_h^N\|_{L^2}$	Order	$\|\boldsymbol{u}^N - \boldsymbol{u}_h^N\|_{L^2}$	Order
$2\pi/10$	1.950×10^{-2}		9.149×10^{-2}	
$2\pi/20$	2.164×10^{-3}	3.17	9.573×10^{-3}	3.26
$2\pi/40$	2.703×10^{-4}	3.00	1.195×10^{-3}	3.00

Table 4: $\eta = 0.1, \eta_2 = 0.001, \mu = \mu_0 = 1$

5.2 Energy stability test

Finally, we carry out the numerical experiment to verify the discrete energy stability, and choose the initial data as

$$\begin{aligned} \boldsymbol{u}_1 = \boldsymbol{u}_0 &= \begin{pmatrix} \sin^2 x \sin(2y) \\ -\sin(2x)\sin^2 y \end{pmatrix}, \\ \boldsymbol{H}_1 = \boldsymbol{H}_0 &= \begin{pmatrix} -\sin y \cos x \\ \sin x \cos y \end{pmatrix}, \\ p_0 &= \sin(2x)\sin(2y). \end{aligned}$$

The time step size and the spatial resolution are given by $\tau = 0.1$ and $h = 1/20$, respectively. The discrete energy function is defined in Theorem 3.4. We still adopt the quadratic elements for $(\boldsymbol{H}, \boldsymbol{u})$ and linear elements for p. The energy evolution curve is displayed in Figure 1, up to a final time $T = 10$, which indicates a clear energy decay.

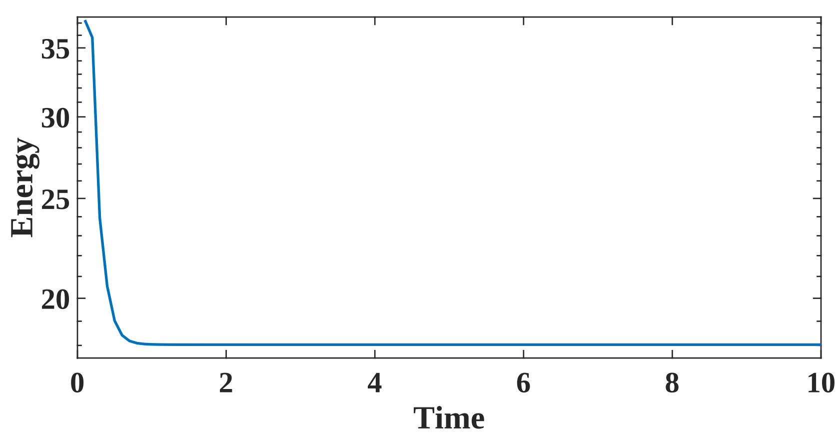

Figure 1: Discrete energy evolution of the incompressible resistive MHD system

6 Conclusion

In this work we have designed a fully decoupled second-order BDF scheme, combined with the mixed FEM spatial approximation, for the incompressible resistive MHD system (1.1)-(1.3). The unconditional energy stability, unique solvability and optimal rate error estimate have been established at a theoretical level. The fully decoupled method adopted in this work is an efficient approach to deal with the incompressible constraint and nonlinear terms, and therefore the technique could be applied to the other incompressible flow system, for example, the multi-phase MHD system.

Acknowledgments

The research of C. Wang was supported in part by NSF DMS-2012269 and NSF DMS-2309548. The research of Z. Xia was supported in part by NSFC-11871139.

References

[1] J. H. Adler, M. Brezina, T. A. Manteuffel, S. F. McCormick, J. W. Ruge, and L. Tang. Island coalescence using parallel first-order system least squares on incompressible resistive magnetohydrodynamics. *SIAM J. Sci. Comput.*, 35(5):S171–S191, 2013.

[2] J. H. Adler, T. A. Manteuffel, S. F. McCormick, and J. W. Ruge. First-order system least squares for incompressible resistive magnetohydrodynamics. *SIAM J. Sci. Comput.*, 32(1):229–248, 2010.

[3] J. H. Adler, T. A. Manteuffel, S. F. McCormick, J. W. Ruge, and G. D. Sanders. Nested iteration and first-order system least squares for incompressible, resistive magnetohydrodynamics. *SIAM J. Sci. Comput.*, 32(3):1506–1526, 2010.

[4] S. Brenner and L. Scott. *The Mathematical Theory of Finite Element Methods*. Springer-Verlag, New York, NY, 2002.

[5] G. Chen, J. Cui, and L. Xu. Analysis of a hybridizable discontinuous galerkin method for the maxwell operator. *ESAIM Math. Model. Numer. Anal.*, 53(1):301–324, 2019.

[6] G. Chen, J. Cui, and L. Xu. A Hybridizable Discontinuous Galerkin Method for the Quad-Curl Problem. *J. Sci. Comput.*, 87(1):16, 2021.

[7] G. Chen, W. Qiu, and L. Xu. Analysis of an interior penalty DG method for the quad-curl problem. *IMA J. Numer. Anal.*, 41(4):2990–3023, 2021.

[8] H. S. Chen and Q. Lin. A high accuracy analysis of the mixed finite element method for biharmonic equations. *Systems Sci. Math. Sci.*, 5(4):352–364, 1992.

[9] W. Chen, X. Wang, Y. Yan, and Z. Zhang. A second order BDF numerical scheme with variable steps for the Cahn-Hilliard equation. *SIAM J. Numer. Anal.*, 57(1):495–525, 2019.

[10] K. Cheng, W. Feng, C. Wang, and S.M. Wise. An energy stable fourth order finite difference scheme for the Cahn-Hilliard equation. *J. Comput. Appl. Math.*, 362:574–595, 2019.

[11] K. Cheng, C. Wang, and S.M. Wise. An energy stable fourier pseudo-spectral numerical scheme for the square phase field crystal equation. *Commun. Comput. Phys.*, 26:1335–1364, 2019.

[12] Q. Cheng and C. Wang. Error estimate of a second order accurate scalar auxiliary variable (SAV) scheme for the thin film epitaxial equation. *Adv. Appl. Math. Mech.*, 13:1318–1354, 2021.

[13] P. G. Ciarlet and P.-A. Raviart. A mixed finite element method for the biharmonic equation. In *Mathematical aspects of finite elements in partial differential equations*, Publication No. 33, pages 125–145. Math. Res. Center, Univ. of Wisconsin-Madison, Academic Press, New York, 1974.

[14] P.G. Ciarlet and P. Raviart. General Lagrange and Hermite interpolation in $\mathbf{R}^n$ with applications to finite element methods. *Arch. Rational Mech. Anal.*, 46:177–199, 1972.

[15] B. Cockburn and C.-W. Shu. The local discontinuous Galerkin method for time-dependent convection-diffusion systems. *SIAM J. Numer. Anal.*, 35(6):2440–2463, 1998.

[16] P.A. Davidson. *An introduction to magnetohydrodynamics.* Cambridge University Press, Cambridge, 2001.

[17] L. Dong, C. Wang, H. Zhang, and Z. Zhang. A positivity-preserving second-order bdf scheme for the Cahn-Hilliard equation with variable interfacial parameters. *Commun. Comput. Phys.*, 28:967–988, 2020.

[18] H.-Y. Duan, R. C. E. Tan, S.-Y. Yang, and C.-S. You. A mixed H^1-conforming finite element method for solving Maxwell's equations with non-H^1 solution. *SIAM J. Sci. Comput.*, 40(1):A224–A250, 2018.

[19] W. Feng, C. Wang, S.M. Wise, and Z. Zhang. A second-order energy stable Backward Differentiation Formula method for the epitaxial thin film equation with slope selection. *Numer. Methods Partial Differ. Equ.*, 34(6):1975–2007, 2018.

[20] H. Gao and W. Qiu. A semi-implicit energy conserving finite element method for the dynamical incompressible magnetohydrodynamics equations. *Comput. Methods Appl. Mech. Engrg.*, 346:982–1001, 2019.

[21] V. Girault and P. Raviart. *Finite Element Method for Navier–Stokes Equations: Theory and Algorithms.* Springer-Verlag, Berlin, Herdelberg, 1987.

[22] M.D. Gunzburger, A.J. Meir, and J.S. Peterson. On the existence, uniqueness, and finite element approximation of solutions of the equations of stationary, incompressible magnetohydrodynamics. *Math. Comp.*, 56(194):523–563, 1991.

[23] C. He and Y. Wang. On the regularity criteria for weak solutions to the magnetohydrodynamic equations. *J. Differ. Equ.*, 238(1):1–17, 2007.

[24] Y. He. Unconditional convergence of the Euler semi-implicit scheme for the three-dimensional incompressible MHD equations. *IMA J. Numer. Anal.*, 35(2):767–801, 2015.

[25] Y. He and J. Zou. *A priori* estimates and optimal finite element approximation of the MHD flow in smooth domains. *M2AN Math. Model. Numer. Anal.*, 52(1):181–206, 2018.

[26] Q. Hong, J. Hu, S. Shu, and J. Xu. A discontinuous Galerkin method for the fourth-order curl problem. *J. Comput. Math.*, 30(6):565–578, 2012.

[27] K. Hu, Q. Zhang, and Z. Zhang. Simple curl-curl-conforming finite elements in two dimensions. *SIAM J. Sci. Comput.*, 42(6):A3859–A3877, 2020.

[28] J. Jin. *The finite element method in electromagnetics.* Wiley-Interscience [John Wiley & Sons], New York, second edition, 2002.

[29] J. J. Lee, S. J. Shannon, T. Bui-Thanh, and J. N. Shadid. Analysis of an HDG method for linearized incompressible resistive MHD equations. *SIAM J. Numer. Anal.*, 57(4):1697–1722, 2019.

[30] B. Li, J. Wang, and L. Xu. A convergent linearized Lagrange finite element method for the magnetohydrodynamic equations in two-dimensional nonsmooth and nonconvex domains. *SIAM J. Numer. Anal.*, 58(1):430–459, 2020.

[31] F. Li and L. Xu. Arbitrary order exactly divergence-free central discontinuous Galerkin methods for ideal MHD equations. *J. Comput. Phys.*, 231(6):2655–2675, 2012.

[32] L. Li, D. Zhang, and W. Zheng. A constrained transport divergence-free finite element method for incompressible MHD equations. *J. Comput. Phys.*, 428:Paper No. 109980, 22, 2021.

[33] S. Li. A fourth-order divergence-free method for MHD flows. *J. Comput. Phys.*, 229(20):7893–7910, 2010.

[34] W. Li, W. Chen, C. Wang, Y. Yan, and R. He. A second order energy stable linear scheme for a thin film model without slope selection. *J. Sci. Comput.*, 76:1905–1937, 2018.

[35] X. Li, W. Wang, and J. Shen. Stability and error analysis of IMEX SAV schemes for the magnetohydrodynamic equations. *SIAM J. Numer. Anal.*, 60(3):1026–1054, 2022.

[36] F. Lin, L. Xu, and P. Zhang. Global small solutions of 2-D incompressible MHD system. *J. Differ. Equ.*, 259(10):5440–5485, 2015.

[37] F. Lin and P. Zhang. Global small solutions to an MHD-type system: The three-dimensional case. *Comm. Pure Appl. Math.*, 67(4):531–580, 2014.

[38] C. Liu, J. Shen, and X. Yang. Decoupled energy stable schemes for a phase-field model of two-phase incompressible flows with variable density. *J. Sci. Comput.*, 62(2):601–622, 2015.

[39] X. Meng, Z. Qiao, C. Wang, and Z. Zhang. Artificial regularization parameter analysis for the no-slope-selection epitaxial thin film model. *CSIAM Trans. Appl. Math.*, 1(3):441–462, 2020.

[40] P. Monk. A mixed finite element method for the biharmonic equation. *SIAM J. Numer. Anal.*, 24(4):737–749, 1987.

[41] J.-C. Nédélec. A new family of mixed finite elements in $\mathbf{R}^3$. *Numer. Math.*, 50(1):57–81, 1986.

[42] J. Pyo and J. Shen. Normal mode analysis of second-order projection methods for incompressible flows. *Discrete Contin. Dyn. Syst. Ser. B*, 5(3):817–840, 2005.

[43] J. Sun. A mixed FEM for the quad-curl eigenvalue problem. *Numer. Math.*, 132(1):185–200, 2016.

[44] V. Thomée. *Galerkin Finite Element Methods for Parabolic Problems*. Springer-Verlag, Berlin, 2006.

[45] Y. Unger, M. Mond, and H. Branover. *Liquid Metal Flows: Magnetohydrodynamics and Application*. 1988.

[46] C. Wang and J.-G. Liu. Convergence of gauge method for incompressible flow. *Math. Comp.*, 69(232):1385–1407, 2000.

[47] C. Wang, J. Wang, Z. Xia, and L. Xu. Optimal error estimates of a Crank–Nicolson finite element projection method for magnetohydrodynamic equations. *ESAIM Math. Model. Numer. Anal.*, 56(3):767–789, 2022.

[48] L. Xu and P. Zhang. Global small solutions to three-dimensional incompressible magnetohydrodynamical system. *SIAM J. Math. Anal.*, 47(1):26–65, 2015.

[49] Y. Xu and C.-W. Shu. Local discontinuous Galerkin methods for high-order time-dependent partial differential equations. *Commun. Comput. Phys.*, 7(1):1–46, 2010.

[50] J. Yan and C.-W. Shu. A local discontinuous Galerkin method for KdV type equations. *SIAM J. Numer. Anal.*, 40(2):769–791, 2002.

[51] Y. Yan, W. Chen, C. Wang, and S.M. Wise. A second-order energy stable BDF numerical scheme for the Cahn-Hilliard equation. *Commun. Comput. Phys.*, 23:572–602, 2018.

[52] J. Yang, S. Mao, X. He, X. Yang, and Y. He. A diffuse interface model and semi-implicit energy stable finite element method for two-phase magnetohydrodynamic flows. *Comput. Methods Appl. Mech. Engrg.*, 356:435–464, 2019.

[53] X. Yang. Efficient and energy stable scheme for the hydrodynamically coupled three components Cahn-Hilliard phase-field model using the stabilized-Invariant Energy Quadratization (S-IEQ) Approach. *J. Comput. Phys.*, 438:110342, 24, 2021.

[54] X. Yang. A new efficient fully-decoupled and second-order time-accurate scheme for Cahn-Hilliard phase-field model of three-phase incompressible flow. *Comput. Methods Appl. Mech. Engrg.*, 376:113589, 27, 2021.

[55] X. Yang. A novel decoupled second-order time marching scheme for the two-phase incompressible Navier-Stokes/Darcy coupled nonlocal Allen-Cahn model. *Comput. Methods Appl. Mech. Engrg.*, 377:113597, 26, 2021.

[56] X. Yang. A novel fully-decoupled, second-order time-accurate, unconditionally energy stable scheme for a flow-coupled volume-conserved phase-field elastic bending energy model. *J. Comput. Phys.*, 432:110015, 26, 2021.

[57] X. Yang. On a novel fully decoupled, second-order accurate energy stable numerical scheme for a binary fluid-surfactant phase-field model. *SIAM J. Sci. Comput.*, 43(2):B479–B507, 2021.

[58] X. Yang, G.-D. Zhang, and X. He. Convergence analysis of an unconditionally energy stable projection scheme for magneto-hydrodynamic equations. *Appl. Numer. Math.*, 136:235–256, 2019.

[59] M. Yuan, W. Chen, C. Wang, S.M. Wise, and Z. Zhang. A second order accurate in time, energy stable finite element scheme for the Flory-Huggins-Cahn-Hilliard equation. *Adv. Appl. Math. Mech.*, 14(6):1477–1508, 2022.

[60] G.-D. Zhang, X. He, and X. Yang. A decoupled, linear and unconditionally energy stable scheme with finite element discretizations for magneto-hydrodynamic equations. *J. Sci. Comput.*, 81(3):1678–1711, 2019.

[61] G.-D. Zhang, X. He, and X. Yang. Decoupled, linear, and unconditionally energy stable fully discrete finite element numerical scheme for a two-phase ferrohydrodynamics model. *SIAM J. Sci. Comput.*, 43(1):B167–B193, 2021.

[62] G.-D. Zhang, X. He, and X. Yang. A fully decoupled linearized finite element method with second-order temporal accuracy and unconditional energy stability for incompressible MHD equations. *J. Comput. Phys.*, 448:Paper No. 110752, 19, 2022.

[63] Q. Zhang, L. Wang, and Z. Zhang. $H(\mathrm{curl}^2)$-conforming finite elements in 2 dimensions and applications to the quad-curl problem. *SIAM J. Sci. Comput.*, 41(3):A1527–A1547, 2019.

[64] J. Zhao, X. Yang, J. Shen, and Q. Wang. A decoupled energy stable scheme for a hydrodynamic phase-field model of mixtures of nematic liquid crystals and viscous fluids. *J. Comput. Phys.*, 305:539–556, 2016.

[65] B. Zheng, Q. Hu, and J. Xu. A nonconforming finite element method for fourth order curl equations in $\mathbb{R}^3$. *Math. Comp.*, 80(276):1871–1886, 2011.